Available online at www.sciencedirect.com
ScienceDirect
International Journal of Multiphase Flow 33 (2007) 252–281
International Journal of Multiphase Flow
www.elsevier.com/locate/ijmulflow

Modeling droplet dispersion and interphase turbulent kinetic energy transfer using a new dual-timescale Langevin model

M.G. Pai, S. Subramaniam *

Department of Mechanical Engineering, 3020, H.M. Black Engineering, Iowa State University, Ames, IA 50011, USA

Received 19 May 2006; received in revised form 7 August 2006

Abstract

Dispersion of spray droplets and the modulation of turbulence in the ambient gas by the dispersing droplets are two coupled phenomena that are closely linked to the evolution of global spray characteristics, such as the spreading rate of the spray and the spray cone angle. Direct numerical simulations (DNS) of turbulent gas flows laden with sub-Kolmogorov size particles, in the absence of gravity, report that dispersion statistics and turbulent kinetic energy (TKE) evolve on different timescales. Furthermore, each timescale behaves differently with Stokes number, a non-dimensional flow parameter (defined in this context as the ratio of the particle response time to the Kolmogorov timescale of turbulence) that characterizes how quickly a particle responds to turbulent fluctuations in the carrier or gas phase. A new dual-timescale Langevin model (DLM) composed of two coupled Langevin equations for the fluctuating velocities, one for each phase, is proposed. This model possesses a unique feature that the implied TKE and velocity autocorrelation in each phase evolve on different timescales. Consequently, this model has the capability of simultaneously predicting the disparate Stokes number trends in the evolution of dispersion statistics, such as velocity autocorrelations, and TKE in each phase. Predictions of dispersion statistics and TKE from the new model show good agreement with published DNS of non-evaporating and evaporating droplet-laden turbulent flow.
© 2006 Elsevier Ltd. All rights reserved.

Keywords: Multiphase flow; Multiscale; Langevin model; Turbulence; Dispersion; Stokes number; Droplets; Velocity autocorrelation

1. Background

The evolution of a fuel spray in an internal combustion engine is strongly influenced by its interaction with the rapidly changing turbulent gas phase in the combustion chamber. Turbulence in the ambient gas directly affects the spreading rate of a spray which in turn affects the spray penetration length and spray cone angle. Dispersing droplets in turn amplify or suppress the turbulence in the ambient gas, thereby coupling the effects of turbulence and droplet dispersion.

* Corresponding author. Tel.: +1 515 294 3698; fax: +1 515 294 3261.
E-mail address: shankar@iastate.edu (S. Subramaniam).

0301-9322/$ - see front matter © 2006 Elsevier Ltd. All rights reserved.
doi:10.1016/j.ijmultiphaseflow.2006.08.007

Direct numerical simulations (DNS) of decaying particle-laden turbulence performed in the absence of gravity report that the timescale for interphase turbulent kinetic energy (TKE) transfer is different from the timescale associated with particle dispersion, and that the trends of these timescales are also different for varying Stokes numbers. Particles with high Stokes number lose energy *faster* than particles with low Stokes number in freely decaying turbulence (Sundaram and Collins, 1999). On the other hand, particles with high Stokes number lose correlation with their initial velocities *slower* than particles with low Stokes number in stationary turbulence (Mashayek et al., 1997; Squires and Eaton, 1991). The disparate behavior of the velocity autocorrelation and TKE timescales affects the dispersion characteristics of a spray. Turbulence models for spray computations (or particle-laden turbulent flows, in general) must be capable of simultaneously capturing these disparate timescale trends with Stokes number, in order to be predictive.

Experimental evidence for the dependence of the evolution timescales of velocity autocorrelation and interphase TKE transfer on Stokes number is available in the literature (Snyder and Lumley, 1971; Wells and Stock, 1983; Groszmann and Rogers, 2004). However, unlike in the DNS studies, it is difficult to isolate physical mechanisms that affect these timescales in experiments. Also given the uncertainty involved in experiments in extracting velocity autocorrelations and TKE in dispersed two-phase flows, the canonical DNS cited earlier are of intrinsic value to the modeling community for two principal reasons. Firstly, crossing trajectory effects due to particle drift, and particle inertia effects are easily isolated in numerical computations. Secondly, models for individual terms in the governing equations for dispersed two-phase flows, like the interphase TKE and mass transfer, can be tested in isolation by comparing with corresponding terms extracted from DNS. The same is not possible with experiments. Thus, reproducing results from such canonical two-phase DNS constitutes an important first step in validating multiphase flow turbulence models.

In the Lagrangian–Eulerian (LE) representation of two-phase flows, the dispersed phase is modeled using *computational* particles whose velocities evolve according to a drag model of the form

$$\frac{\mathrm{d}\mathbf{V}_\mathrm{p}}{\mathrm{d}t} = \frac{\mathbf{U}_\mathrm{f} - \mathbf{V}_\mathrm{p}}{\tau_\mathrm{p}} C_\mathrm{d}(Re_\mathrm{d}) + \mathbf{F}_\mathrm{add}, \tag{1}$$

and whose positions evolve according to

$$\frac{\mathrm{d}\mathbf{X}_\mathrm{p}}{\mathrm{d}t} = \mathbf{V}_\mathrm{p}, \tag{2}$$

where $\mathbf{V}_\mathrm{p}$ is the instantaneous particle velocity, $\mathbf{U}_\mathrm{f}$ is the instantaneous gas-phase velocity,[1] $\tau_\mathrm{p} = (\rho_\mathrm{d} d_\mathrm{p}^2)/(\rho_\mathrm{f} 18 \nu_\mathrm{f})$ is the particle response timescale, $\mathbf{X}_\mathrm{p}$ is the particle position and $\mathbf{F}_\mathrm{add}$ represents additional terms that include lift and body forces. The instantaneous gas-phase velocity $\mathbf{U}_\mathrm{f}$ is decomposed into a mean $\langle \mathbf{U}_\mathrm{f} \rangle$ and a fluctuating component $\mathbf{u}'_\mathrm{f}$. Here, ρ_d and ρ_f are the thermodynamic densities of the dispersed phase and fluid phase, respectively, d_p is the particle or droplet diameter and ν_f is the kinematic viscosity of the fluid phase. A drag coefficient C_d that depends on the droplet Reynolds number Re_d is generally included as shown. The major research effort in modeling turbulent two-phase flows using the LE representation has been directed towards arriving at a suitable model for $\mathbf{U}_\mathrm{f}$. The principal LE modeling studies that are relevant to dispersion and TKE evolution are reviewed here.

Lu (1995) uses a time-series analysis involving fluid-phase temporal and spatial Eulerian velocity correlations to arrive at a stochastic model for the fluid velocity at the particle location, in the limit of one-way coupled turbulence. Spray droplet interactions with the gas phase are, however, strongly two-way coupled. Nevertheless, testing the behavior of a two-phase model in the limit of one-way coupled spray configurations is indeed necessary. Lu reports good agreement between model results and theoretical results of Csanady (1963), and particle-laden grid-generated turbulence results of Snyder and Lumley (1971) in predicting particle diffusion coefficients and velocity autocorrelations. Mashayek (1999) used Lu's time-series approach to predict particle-velocity autocorrelation functions and asymptotic diffusion coefficients for non-evaporating and evaporating droplets laden in one-way coupled stationary turbulence, again reporting overall reasonable agreement with DNS data (Mashayek et al., 1997). An extension of the time-series model has been tested by Gao and Mashayek (2004b) in compressible homogeneous shear flows with interphase mass transfer due to

[1] Also sometimes referred to as the gas-phase velocity "seen" by the particles.

evaporating droplets. They report good agreement of predicted droplet velocity correlations and droplet-fluid velocity cross-correlations with DNS of evaporating droplets in a low Mach number turbulent shear flow (Mashayek, 1998). Pozorski and Minier (1999) modified the Lagrangian integral timescale in the generalized Langevin model proposed by Haworth and Pope (1986) to arrive at the fluid velocity "seen" by the particles. To our knowledge, no validation tests are available in the literature that quantify the predictive capability of this model in canonical particle-laden flows. Chagras et al. (2005) employ a Langevin-type equation that uses the Lagrangian integral timescale of the fluid "seen" by the particles and the fluid-phase Reynolds stresses to arrive at a model for $\mathbf{u}_f'$. They analyze several cases of two-way coupled gas–solid pipe flow with large mass loading and report overall agreement of temperature profiles and instantaneous velocities with experimental results. Chen and Pereira (1997) use an assumed probability density function (pdf) for the spatial distribution of the particles whose variance evolves in time by an ordinary differential equation containing an assumed fluid-phase Lagrangian velocity autocorrelation of the Frenkiel form (Gouesbet and Berlemont, 1999). They report good match of predicted dispersed-phase velocities from their two-way coupled simulations with results from experiments conducted on particle-laden planar mixing layers and co-flowing planar jets.

With the exception of Mashayek (1999), there is no evidence in the literature of tests conducted with the aforementioned models in simple canonical two-phase flows (such as stationary or freely decaying particle-laden turbulence) to test their capability in simultaneously capturing the energy and dispersion timescales as observed in DNS. However, the time series model (Lu, 1995) used by Mashayek (1999) relies on statistics of the fluid phase that are valid only in the limit of one-way coupled two-phase flows. Extending the time series model to two-phase flows with significant two-way coupling effects will require the knowledge of the Eulerian spatial correlation of gas-phase velocity which is a non-trivial quantity to measure or model in such flows. Also, the extension of the time-series model proposed by Gao and Mashayek (2004a,b) involves correlations among the velocity components, temperature and mass fraction, with the assumption that all these correlations evolve on the same Eulerian fluid integral timescale.

Another common feature of the LE models cited above is the use of the particle response time τ_p as the timescale for both interphase momentum and TKE transfer. Recently, a representative LE model (Amsden et al., 1989) was tested in freely decaying turbulence laden with sub-Kolmogorov size particles (Pai and Subramaniam, 2006). It was shown in that study that LE models based on the particle response timescale fail to accurately capture trends in the evolution of TKE in both phases with varying Stokes numbers, when tested in the canonical problem. This observation pointed to a need for improvement in the predictive capability of existing LE models. A multiscale interaction timescale to replace τ_p was proposed (Pai and Subramaniam, 2006) that captured trends in the evolution of TKE with varying Stokes number as seen in the DNS.

The primary objective of this work is to propose a new model called the dual-timescale Langevin model (DLM). In this model, we adopt a Lagrangian–Lagrangian description of both the fluid and dispersed phases. Unlike the models cited earlier, we do not use Eq. (1) to evolve the particle velocities, and also the implied TKE in either phase evolves on a timescale derived by taking into account the multiscale nature of droplet-turbulence interaction (Pai and Subramaniam, 2006). Furthermore, the novel feature of this model is the existence of dual timescales in a single model that enables the model to *simultaneously* capture the disparate Stokes number trends in the evolution of TKE and also particle dispersion characteristics in both phases. It is important to note that although Langevin models have been successful in predicting turbulent reactive flows (Pope, 2000, 1985), extending these models to two-phase flows is not straightforward. This is because single-phase Langevin models are based on a single timescale and such models are clearly incapable of simultaneously capturing the disparate timescales of TKE and autocorrelation observed in two-phase DNS. However, Langevin models have the advantage that they are more amenable to analysis than existing LE models based on stochastic white noise (Gosman and Ioannides, 1983; Amsden et al., 1989). A second objective of this work, and a guiding principle for the model development, is to clearly identify terms in the governing equations of the dispersed phase that require modeling.

The rest of the paper is organized as follows. The new stochastic model is introduced and implied evolution equations for the statistics of the fluid and dispersed phases are derived in Section 2. A new hypothesis for modeling the interphase TKE transfer called the Equilibration of Energy (EoE) concept is presented in Section 3. The rationale underlying the specification of model constants is explained in Section 4. Test cases for which DNS data are available from Mashayek et al. (1997) for both non-evaporating and evaporating droplet-laden

stationary turbulence are described in Section 5. Model predictions for these test cases are reported in Section 6. An assessment of the model and the DNS data are presented in Section 7. The final section presents the principal conclusions of the study.

2. Dual-timescale Langevin model (DLM)

A new stochastic model called the dual-timescale Langevin model (DLM) is proposed for homogeneous turbulent two-phase flows. This model consists of a system of stochastic differential equations (SDE) for the modeled fluctuating Lagrangian gas-phase velocity **u** and fluctuating Lagrangian dispersed-phase velocity **v**. The proposed system of SDEs is

$$\mathrm{d}u_i = -\left[\frac{1}{2\tau_1} + \left(\frac{1}{2} + \frac{3}{4}C_0\right)\frac{\varepsilon_\mathrm{f}}{k_\mathrm{f}}\right]u_i\mathrm{d}t + \left[C_0\varepsilon_\mathrm{f} + \frac{2}{3}\frac{k_\mathrm{f}}{\tau_1} + \frac{2}{3}\left(\frac{k_\mathrm{f}^\mathrm{e} - k_\mathrm{f}}{\tau_2}\right)\right]^{1/2}\mathrm{d}W_i^u \tag{3}$$

$$\mathrm{d}v_i = -\frac{1}{2\tau_3}v_i\mathrm{d}t + \left[\frac{2}{3}\frac{k_\mathrm{d}}{\tau_3} + \frac{2}{3}\left(\frac{k_\mathrm{d}^\mathrm{e} - k_\mathrm{d}}{\tau_4}\right)\right]^{1/2}\mathrm{d}W_i^v, \tag{4}$$

where τ_1, τ_2, τ_3 and τ_4 are timescales that appear in the drift and diffusion coefficients[2] of each SDE, while $\mathrm{d}W_i^u$ and $\mathrm{d}W_i^v$ are independent Wiener processes (Kloeden and Platen, 1992). The subscript i denotes the Cartesian components. The TKE in the dispersed phase is denoted k_d and the TKE in the gas phase is denoted k_f with a superscript 'e' to denote their 'equilibrium' values (the concept of 'equilibrium' is explained in Section 3).[3] Also, ε_f is the gas-phase dissipation enhanced by the presence of the dispersed phase. The constant $C_0 = 2.1$, which is identical to that used in the Simplified Langevin model (SLM) (Pope, 2000). Mean velocity and, hence mean slip in either phase is assumed to be zero for simplicity, although this is not an inherent limitation of DLM. The fluid-phase SDE can be viewed as an extension of the SLM (Pope, 2000; Haworth and Pope, 1986) to two-phase flows, but with an important difference being the introduction of drift and diffusion timescales that are different from each other. Also, additional terms involving k_f^e and k_d^e (in parentheses) that represent interphase interactions have been added. The coupling between the two phases is only through moments of the velocities in each phase like TKE (k_f and k_d) and the dissipation ε_f, and not explicitly through the instantaneous values of u_i and v_i.

One can derive the implied evolution equations for the TKE in the fluid phase, defined as $k_\mathrm{f} = (1/2)\langle u_i u_i\rangle$ (where the averaging is performed over an ensemble of realizations) and the TKE in the dispersed phase, defined as $k_\mathrm{d} = (1/2)\langle v_i v_i\rangle$, from Eqs. (3) and (4), respectively, to be

$$\frac{\mathrm{d}k_\mathrm{f}}{\mathrm{d}t} = \left(\frac{k_\mathrm{f}^\mathrm{e} - k_\mathrm{f}}{\tau_2}\right) - \varepsilon_\mathrm{f} \tag{5}$$

$$\frac{\mathrm{d}k_\mathrm{d}}{\mathrm{d}t} = \left(\frac{k_\mathrm{d}^\mathrm{e} - k_\mathrm{d}}{\tau_4}\right). \tag{6}$$

Of the four timescales present in Eqs. (3) and (4), only τ_2 and τ_4 appear in the above equations. The equilibrium energies, k_f^e and k_d^e, are related to each other as will be shown later, and so the evolution of k_f and k_d are coupled through these terms. It has to be emphasized here that the interphase TKE transfer timescales τ_2 and τ_4 are not *equal* to τ_p although they do depend on this timescale. Note that for widely-used LE models, the interphase TKE transfer evolves on the particle response timescale τ_p which was found to be inadequate to capture the multiscale nature of particle–turbulence interaction (Pai and Subramaniam, 2006). The exact form of these timescales will be presented in Section 4.

2.1. Stationary turbulence limit

In the context of two-phase flows, an important canonical problem is homogeneous turbulence in which the fluid phase turbulence is artificially forced to remain stationary, while the dispersed phase evolves to its

[2] The terms 'drift' and 'diffusion' are used in the sense of stochastic differential equation theory.

[3] The subscript f stands for the gas phase or fluid phase, and the subscript d stands for the dispersed phase.

stationary state. Several studies have been performed in this important limiting case using DNS (Squires and Eaton, 1991; Mashayek et al., 1997), making it an ideal case for model validation.

In the limit of stationary turbulence, the drift coefficient in the fluid phase SDE in Eq. (3) is modified along the lines of the SLM proposed for single-phase stationary turbulence (Pope, 2000) as

$$\mathrm{d}u_i = -\left(\frac{1}{2\tau_1}+\frac{3}{4}C_0\frac{\varepsilon_\mathrm{f}}{k_\mathrm{f}}\right)u_i\mathrm{d}t + \left[C_0\varepsilon_\mathrm{f}+\frac{2}{3}\frac{k_\mathrm{f}}{\tau_1}+\frac{2}{3}\left(\frac{k_\mathrm{f}^\mathrm{e}-k_\mathrm{f}}{\tau_2}\right)\right]^{1/2}\mathrm{d}W_i^u. \tag{7}$$

With this modification, the fluid phase dissipation drops out of the implied evolution equation for the TKE in the fluid phase, which now reads

$$\frac{\mathrm{d}k_\mathrm{f}}{\mathrm{d}t} = \left(\frac{k_\mathrm{f}^\mathrm{e}-k_\mathrm{f}}{\tau_2}\right). \tag{8}$$

In the limit of two-way coupled homogeneous particle-laden stationary turbulence, Eqs. (8) and (6) form the modeled governing equations for the TKE in the fluid and dispersed phases, respectively. The only term appearing on the right-hand side of these equations is the TKE transfer due to inter-phase interactions.

Eq. (8) is a physically consistent model for k_f in an artificially forced two-phase flow system where energy is added at the large scales to exactly balance the viscous dissipation, which now includes additional dissipation due to the presence of the particles in the fluid phase. DLM predicts that, in the case of stationary turbulence, the TKE in the fluid phase would evolve to an equilibrium value k_f^e over a timescale τ_2. Statistics related to dispersion of spray droplets, as implied by DLM, are derived next.

2.2. Implied Lagrangian velocity autocorrelation

In stationary isotropic turbulence, which is the main focus of this study, the Lagrangian velocity autocorrelation denoted $R_{\beta_{ij}}(s)$ is given as (Hinze, 1975)

$$R_{\beta_{ij}}(s) = \frac{\langle\gamma_i(t_0)\gamma_j(t_0+s)\rangle}{\langle\gamma_i(t_0)\gamma_j(t_0)\rangle}, \tag{9}$$

where t_0 can be any initial time after the system reaches stationarity and s is the *separation* time. No summation is implied over repeated indices. Here, γ stands for either u or v. The Lagrangian autocorrelation is simply a normalized autocovariance and gives a measure of how quickly the fluid particle or droplet loses correlation with its velocity at some earlier time. Note that for isotropic turbulence, $R_{\beta_{ij}} = 0$, for $i \neq j$, and $R_{\beta_{ii}} = R_{\beta_{jj}}$, for $i = j = \{1,2,3\}$.

The evolution equation for the fluid velocity autocovariance implied by DLM for the stationary case is

$$\frac{\mathrm{d}\langle u_i(t_0)u_j(t)\rangle}{\mathrm{d}t} = -\left(\frac{1}{2\tau_1}+\frac{3}{4}C_0\frac{\varepsilon_\mathrm{f}}{k_\mathrm{f}}\right)\langle u_i(t_0)u_j(t)\rangle, \tag{10}$$

while the evolution equation for the dispersed-phase velocity autocovariance is

$$\frac{\mathrm{d}\langle v_i(t_0)v_j(t)\rangle}{\mathrm{d}t} = -\frac{1}{2\tau_3}\langle v_i(t_0)v_j(t)\rangle, \tag{11}$$

where $t = t_0 + s$.

A striking feature of DLM is that Eqs. (5) and (6) depend on the timescales τ_2 and τ_4, respectively, while Eqs. (10) and (11) depend on timescales τ_1 and τ_3, respectively. In DLM, therefore, the evolution of TKE can be constructed to behave *differently* from the evolution of the velocity autocovariance. In model proposals that use the generalized Langevin model (Pozorski and Minier, 1999), however, the implied TKE in the fluid phase and the velocity autocorrelation evolve over the same timescale, namely the Lagrangian integral timescale.

The dispersion of droplets or fluid particles is characterized by the diffusion coefficient tensor associated with phase β, denoted $\alpha_{\beta_{ij}}$. In the isotropic case, the diagonal components of the diffusion coefficient tensor are all identical viz. $\alpha_{\beta_{11}} = \alpha_{\beta_{22}} = \alpha_{\beta_{33}} = \alpha_\beta$. In the stationary case, the diffusion coefficient tensor and the Lagrangian velocity autocorrelation tensor are related by

$$\alpha_{\beta_{ij}}(t) = \langle \gamma_i(t_0)\gamma_j(t_0)\rangle \int_0^t R_{\beta_{ij}}(t')\mathrm{d}t' \tag{12}$$

(again, no summation is implied over repeated indices).

3. Equilibration of energy (EoE) concept

The right-hand sides of Eqs. (8) and (6) are models for the interphase TKE transfer, and are based on the EoE concept that was proposed by Xu and Subramaniam (2006). This concept is briefly reviewed here for the sake of completeness.

In order to explain the EoE concept, the following system of model equations for the evolution of TKE in a dilute homogeneous two-phase flow system (with no interphase mass transfer) is proposed

$$\frac{\mathrm{d}e_\mathrm{f}}{\mathrm{d}t} = \Pi_{k_\mathrm{f}} - \rho_\mathrm{f}\theta_\mathrm{f}\varepsilon_\mathrm{f} \tag{13}$$

$$\frac{\mathrm{d}e_\mathrm{d}}{\mathrm{d}t} = \Pi_{k_\mathrm{d}}, \tag{14}$$

where $\Pi_{k_\mathrm{f}} = (e_\mathrm{f}^\mathrm{e} - e_\mathrm{f})/\tau_\pi$ and $\Pi_{k_\mathrm{d}} = (e_\mathrm{d}^\mathrm{e} - e_\mathrm{d})/\tau_\pi$ are the interphase TKE transfer terms. Here, τ_π is the interphase TKE transfer timescale, while $e_\mathrm{f} = \rho_\mathrm{f}\theta_\mathrm{f}k_\mathrm{f}$ and $e_\mathrm{d} = \rho_\mathrm{d}\theta_\mathrm{d}k_\mathrm{d}$ are the *specific* fluid phase and dispersed phase energies, respectively, and $e_\mathrm{f}^\mathrm{e} = \rho_\mathrm{f}\theta_\mathrm{f}k_\mathrm{f}^\mathrm{e}$ and $e_\mathrm{d}^\mathrm{e} = \rho_\mathrm{d}\theta_\mathrm{d}k_\mathrm{d}^\mathrm{e}$ are the equilibrium *specific* TKEs in the gas phase and dispersed phase, respectively. The volume fractions of the fluid phase and dispersed phase are denoted θ_f and $\theta_\mathrm{d} = 1 - \theta_\mathrm{f}$, respectively. Collisions among particles are elastic and hence no dissipation is considered in the dispersed phase.

Adding Eqs. (13) and (14) results in

$$\frac{\mathrm{d}e_\mathrm{m}}{\mathrm{d}t} = -\rho_\mathrm{f}\theta_\mathrm{f}\varepsilon_\mathrm{f},$$

where $e_\mathrm{m} = \rho_\mathrm{m}k_\mathrm{m} = e_\mathrm{f} + e_\mathrm{d} = \rho_\mathrm{f}\theta_\mathrm{f}k_\mathrm{f} + \rho_\mathrm{d}\theta_\mathrm{d}k_\mathrm{d}$ is the mixture energy in the two-phase flow system and ρ_m is the mixture density defined as $\rho_\mathrm{m} = \rho_\mathrm{d}\theta_\mathrm{d} + \rho_\mathrm{f}\theta_\mathrm{f}$. It is assumed that $\Pi_{k_\mathrm{f}} = -\Pi_{k_\mathrm{d}}$, which implies that the interphase TKE transfer is conservative. This assumption is valid for rigid particle-laden turbulent flows. However, as will be shown later, this assumption can be extended to the droplet-laden turbulent flow considered in this study.

The EoE concept states that if

$$\frac{\mathrm{d}e_\mathrm{m}}{\mathrm{d}t} = -\rho_\mathrm{f}\theta_\mathrm{f}\varepsilon_\mathrm{f} + \mathscr{F}_\mathrm{f} = 0, \tag{15}$$

where $\mathscr{F}_\mathrm{f}$ is the external artificial forcing required to balance the dissipation in order to maintain $\mathrm{d}e_\mathrm{m}/\mathrm{d}t = 0$, then the specific dispersed phase TKE and specific fluid phase TKE evolve to their respective equilibrium values. Note that the modeled dissipation in the carrier phase is the sum of the single-phase dissipation rate and the additional dissipation due to the presence of boundary layers around the dispersed particles.

Equilibrium values of the specific fluid-phase TKE e_f^e and specific dispersed-phase TKE e_d^e are determined by a model constant C_k defined as

$$\frac{e_\mathrm{d}^\mathrm{e}}{e_\mathrm{m}} = C_\mathrm{k}, \qquad \frac{e_\mathrm{f}^\mathrm{e}}{e_\mathrm{m}} = 1 - C_\mathrm{k}. \tag{16}$$

Since C_k represents the fraction of the specific mixture energy present in the dispersed phase at equilibrium, it must lie between zero and unity.

An implicit dependence of C_k on mass loading ϕ of the two-phase system can be deduced by rewriting Eq. (16) as

$$C_\mathrm{k} = \frac{\rho_\mathrm{d}\theta_\mathrm{d}k_\mathrm{d}^\mathrm{e}}{\rho_\mathrm{m}k_\mathrm{m}} = \frac{\rho_\mathrm{d}\theta_\mathrm{d}k_\mathrm{d}^\mathrm{e}}{\rho_\mathrm{f}\theta_\mathrm{f}k_\mathrm{f}^\mathrm{e} + \rho_\mathrm{d}\theta_\mathrm{d}k_\mathrm{d}^\mathrm{e}} = \frac{\phi\frac{k_\mathrm{d}^\mathrm{e}}{k_\mathrm{f}^\mathrm{e}}}{1 + \phi\frac{k_\mathrm{d}^\mathrm{e}}{k_\mathrm{f}^\mathrm{e}}}, \tag{17}$$

where $\phi = \rho_d\theta_d/(\rho_f\theta_f)$ is the mass loading of the two-phase system. The constant C_k can also depend on other non-dimensional quantities that characterize this homogeneous turbulent two-phase flow system such as Stokes number $St_\eta = \tau_p/\tau_\eta$ (where τ_η is the Kolmogorov timescale), particle Reynolds number Re_d, initial k_d/k_f ratio, d_p/η ratio (where η is Kolmogorov length scale of turbulence) and θ_d.

For a constant mass loading ϕ, decreasing Stokes number should drive the dispersed-phase equilibrium TKE closer to the fluid-phase equilibrium TKE and in the limit of zero Stokes number, the two equilibrium energies k_f^e and k_d^e should match. This observation imposes a constraint on C_k in the limiting case of zero Stokes number and from Eq. (17) we find

$$\lim_{St_\eta \to 0} C_k = \frac{\phi}{1+\phi}. \tag{18}$$

The EoE concept can be extended to the case where the turbulence decays in time (no artificial forcing of the mixture energy in the two-phase flow system). However, a model for the dissipation rate needs to be added to the system of equations (cf. Eqs. (13) and (14)), which now reads

$$\begin{aligned}
\frac{de_f}{dt} &= \Pi_{k_f} - \rho_f\theta_f\varepsilon_f \\
\frac{de_d}{dt} &= \Pi_{k_d} \\
\frac{d\varepsilon_f}{dt} &= -C_{\varepsilon 2}\frac{\varepsilon_f^2}{k_f} + C_s\frac{\varepsilon_f}{k_f}\left(\frac{k_f^e - k_f}{\tau_\pi}\right),
\end{aligned}$$

where ε_f is the fluid-phase dissipation evolving according to a modified single-phase ε equation (Xu and Subramaniam, 2006). The model constant C_s is chosen to be 1.5 and $C_{\varepsilon 2}$ is 1.92.

3.1. Applicability of the EoE concept to droplet-laden turbulent flows

3.1.1. Non-evaporating droplets

Certain assumptions, like conservative interphase TKE transfer and zero dissipation in the dispersed phase, that are used in arriving at the model equations Eqs. (13) and (14) for flows with rigid solid particles need to be revisited and carefully understood when applied to non-evaporating droplet-laden flows. For this we take as reference the exact evolution equation for the dispersed-phase TKE using the Eulerian–Eulerian (EE) approach Eq. (A.7) presented in the Appendix A (see Xu (2004) for more details) for a homogeneous two-phase flow. The important terms that appear in this equation are:

(a) the interphase TKE transfer $\langle u''_{d_i}(S_{Md_i} - U_i S_{\rho_d})\rangle$ where S_{Md_i} is the interphase momentum transfer given by Eq. (A.9) in Appendix A, U_i is the instantaneous velocity in the two-phase flow system, and S_{ρ_d} is the interphase mass transfer given by Eq. (A.10) in Appendix A,
(b) contribution to the dispersed phase TKE due to interphase mass transfer $(1/2)\langle u''_{d_i}u''_{d_i}S_{\rho_d}\rangle - \tilde{k}_d\langle S_{\rho_d}\rangle$, where $\tilde{k}_d$ is the density-weighted TKE in the dispersed phase given by Eq. (A.6), and
(c) the term $\langle u''_{d_i}\partial(I_d\tau_{ki}/\partial x_k)\rangle$ that contains the dissipation in the dispersed phase, where u''_{d_i} is the fluctuating velocity with respect to the volume-averaged velocity in the dispersed phase given by Eq. (A.8) in Appendix A, I_d is the indicator function (Drew, 1983) which is unity in the dispersed phase and zero in the fluid phase and $I_d\tau_{ki}$ is the stress tensor in the dispersed phase.

The reader is referred to Appendix A for more details on these terms. For non-evaporating droplets, S_{ρ_d} is zero.

The system is assumed to be dilute so that collisions and coalescence of droplets are neglected. Break-up of droplets is also neglected. Since the focus of this study is on droplets that are smaller than the Kolmogorov length scale, dissipation inside the droplet can be considered negligible as the flow in the interior of such droplets is in the laminar regime. One could, on the other hand, consider a Hill's vortex (Batchelor, 1971; Clift et al., 1978) inside the droplets to get an estimate of the dissipation. If the velocity inside the droplet is assumed

to be composed of only fluctuations, then one can estimate the dissipation $\varepsilon_{d,in}$ inside the droplet using $\varepsilon_{d,in} = 2\nu_f\langle s_{ij}s_{ij}\rangle$, where s_{ij} is the fluctuating strain rate tensor, using the prescribed stream-function for the Hill's vortex (Batchelor, 1971; Clift et al., 1978). It can be shown that the dissipation inside the droplet scales like r^2, where r is the radius of the droplet, implying that dissipation is small for small droplets. Thus, the term $\langle u''_{d_i}\partial(I_d\tau_{ki})/\partial x_k\rangle$ in Eq. (A.7) is assumed to be negligible for non-evaporating droplets in the two-phase flow regime considered here.

Experiments on single droplets in quiescent (Greene et al., 1993; Warnica et al., 1995a) and turbulent gas fields (Warnica et al., 1995b) have reported that, for droplet Reynolds numbers in the range 10^{-3} to 100, and in the absence of drop oscillation or deformation, the drag on droplets is not different from drag on solid spheres in quiescent conditions. The droplet Reynolds numbers in the current study are $\mathcal{O}(1)$ and well within the range of Reynolds numbers explored in the experiments. Under such conditions, the term S_{Md_j} representing the instantaneous interphase momentum transfer, is equal and opposite in both the phases. Under conditions of zero mean slip velocity in either phase, the fluctuating velocity at the droplet surface u''_{d_i} is the same as the fluctuating gas-phase velocity u''_{f_i} at the same location. These arguments allow us to assume that conservative interphase TKE transfer, and hence the EoE hypothesis, is valid for the class of flows laden with non-evaporating droplets analyzed in this study.

3.1.2. Evaporating droplets

To understand the contribution to the TKE in either phase due to interphase mass transfer in evaporating droplet-laden flows, we again resort to the dispersed-phase TKE evolution equation derived using the EE approach Eq. (A.7) in the Appendix A. The term $(S_{Md_i} - U_i S_{\rho_d})$ in the second term on the right-hand side of Eq. (A.7) essentially works out to a stress contribution, namely $-\tau_{ji}\frac{\partial I_d}{\partial x_j}$, at the interface. One can decompose the fluctuating velocity in the dispersed phase u''_{d_i} into a part that is equal to u''_{f_i} and a stochastic part ξ_i (which we assume to be an isotropic Wiener process). Substituting this decomposition into the dispersed-phase TKE evolution equation (cf. Eq. (A.7)), we get

$$\theta_d\rho_d\frac{d}{dt}\tilde{k}_d = \left\langle u''_{d_i}\frac{\partial(I_d\tau_{ki})}{\partial x_k}\right\rangle - \left\langle (u''_{f_i}+\xi_i)\tau_{ji}\frac{\partial I_d}{\partial x_j}\right\rangle + (1/2)\langle u''_{d_i}u''_{d_i}S_{\rho_d}\rangle - \tilde{k}_d\langle S_{\rho_d}\rangle. \tag{19}$$

We assume that the correlation $\langle\xi_i\tau_{ji}\frac{\partial I_d}{\partial x_j}\rangle$ in the second term on the right-hand side of Eq. (19) is zero for the droplet-laden isotropic turbulence considered in this study. With this simplification, the interphase TKE transfer term in the fluid-phase TKE evolution equation is equal and opposite in sign to that in the dispersed-phase TKE evolution equation (cf. Eq. (A.7)), since

$$-\left\langle u''_{f_i}\tau_{ji}\frac{\partial I_d}{\partial x_j}\right\rangle = \left\langle u''_{f_i}\tau_{ji}\frac{\partial I_f}{\partial x_j}\right\rangle.$$

Thus, the interphase TKE transfer is conservative for this two-phase system. Again, based on a similar argument as for non-evaporating droplets, the dissipation inside an evaporating droplet is assumed to be negligible. The other two terms remaining on the right-hand side of the above equation are the interphase mass transfer terms. No special treatment is required for these terms because in DLM or other Lagrangian models for droplets, a model for the droplet vaporization rate in turn implies a model for the interphase mass transfer terms (see Appendix A for more details).

4. Model constants in DLM

4.1. Specification of C_k

The EoE model constant C_k defined in Eq. (17) represents the ratio of specific TKE in the dispersed phase to that in the two-phase mixture. As noted in Section 3, C_k can depend on the mass loading ϕ, Stokes number St_η, droplet Reynolds number Re_d, initial k_d/k_f ratio and the dispersed-phase volume fraction θ_d. The droplet Reynolds numbers considered in this study are of $\mathcal{O}(1)$, dispersed-phase volume fractions are of $\mathcal{O}(10^{-3})$ and the initial k_d/k_f ratio is of $\mathcal{O}(1)$. Hence, the dependence of C_k on these parameters is neglected in this study.

However, if the above non-dimensional parameters vary by an order of magnitude across the test cases considered, we expect that the dependence of C_k on these parameters will need to be taken into account.

The dependence of C_k on mass loading and Stokes number[4] is accounted for in this study. Since the ratio of the equilibrium TKEs k_d^e/k_f^e (cf. Eq. (17)) is not known *a priori*, a model for C_k is required. The following model for C_k is proposed:

$$C_k = \frac{\phi(1-0.1St_\eta)}{1+\phi(1-0.1St_\eta)}. \tag{20}$$

Note that this specification obeys the correct limiting behavior of C_k as $St_\eta \to 0$ (cf. Eq. (18)). Other functional forms of C_k were also considered but the above specification gave the best agreement with the DNS dataset used in this study. In order to improve the model for C_k, carefully controlled DNS of particle-laden turbulent flows that report the fraction of the mixture energy in each phase are required. Also, the DNS should quantify the effect of non-dimensional parameters in a two-phase flow system, as noted earlier, on the fraction of specific TKE in each phase. To the knowledge of the authors, no such DNS datasets are as yet available in the literature.

4.2. Drift timescales in DLM

A novel feature of the proposed DLM is the presence of two different timescales in each SDE for the drift and diffusion terms. The form of the drift timescales τ_1 and τ_3 in Eqs. (3) and (4), respectively, is now developed.

4.2.1. Zero Stokes number limit

In the limit of zero Stokes number, the droplets respond immediately to the surrounding fluid. In this limit, the fluid-phase velocity autocovariance and the dispersed-phase velocity autocovariance must match. Therefore we require that, in the limit of vanishing Stokes number, the timescale τ_3 in Eq. (11) should tend to the evolution timescale of the velocity autocovariance in Eq. (10).

A simple specification for τ_3 is

$$\frac{1}{\tau_3} = 2\left[\frac{1}{2\tau_1} + \left(\frac{1}{2}+\frac{3}{4}C_0\right)\frac{1}{\tau}\right]\frac{1}{1+St_\eta C_3}, \tag{21}$$

where C_3 is a model constant ($C_3 = 0.1$) and $\tau = k_f/\varepsilon_f$ is the fluid-phase eddy turnover timescale. The timescale obeys the limiting behavior as $St_\eta \to 0$ viz.

$$\lim_{St_\eta \to 0}\left\{\left[\frac{1}{2\tau_1} + \left(\frac{1}{2}+\frac{3}{4}C_0\right)\frac{1}{\tau}\right]\frac{1}{1+St_\eta C_3}\right\} = \frac{1}{2\tau_1} + \left(\frac{1}{2}+\frac{3}{4}C_0\right)\frac{1}{\tau}.$$

Currently, particle velocity autocorrelation data for large Stokes number (say, $St_\eta > 10$) is not available from DNS or experiments that can help determine the behavior of τ_3 in the large St_η limit. Although there is no explicit dependence of the timescale τ_3 on mass loading ϕ, we shall show next that the dependence on ϕ does appear through the timescale τ_1.

4.2.2. Zero mass loading limit

In the limit of zero mass loading, the effect of the dispersed-phase on the fluid-phase momentum is negligible (one-way coupling). Regardless of the Stokes number, the fluid timescales remain unaffected by the presence of the dispersed phase and are identical to those seen in a single phase flow. In this limit, the timescale τ_1, which essentially represents the modification to the fluid velocity autocorrelation timescale due to the presence of dispersed phase, should tend to infinity. We require that the drift timescale in Eq. (3) should approach the specification for the single-phase simplified Langevin model (Pope, 2000).

Truesdell and Elghobashi (1994) have reported velocity autocorrelation decay of the fluid particle at the location of the solid particle in their DNS of two-way coupled particle-laden homogeneous turbulence. This

[4] Henceforth, "Stokes number" refers to St_η the Stokes number based on the Kolmogorov timescale, unless mentioned otherwise.

quantity is different from the fluid-velocity autocorrelation given by Eq. (10), and is not sufficient to determine the dependence of τ_1 on ϕ or St_η. Currently, we neglect the dependence of τ_1 on St_η and prescribe τ_1 to be

$$\frac{1}{\tau_1} = \frac{C_1\phi}{\tau},$$

where C_1 is a model constant ($C_1 = 0.5$). This specification obeys the correct limiting behavior as $\phi \to 0$ viz.

$$\lim_{\phi\to 0}\left[\frac{1}{2\tau_1} + \left(\frac{1}{2}+\frac{3}{4}C_0\right)\frac{1}{\tau}\right] = \left(\frac{1}{2}+\frac{3}{4}C_0\right)\frac{1}{\tau}.$$

4.3. Diffusion timescales in DLM

The timescales τ_2 and τ_4 govern the evolution of TKE in each phase (cf. Eqs. (5) and (6)). In accordance with the EoE concept, and to introduce the capability to capture the multiscale nature of a turbulent two-phase mixture into DLM, the timescales τ_2 and τ_4 are chosen to be equal to $\tau_\pi = \langle\tau_{\text{int}}\rangle/C_\pi$, where $\langle\tau_{\text{int}}\rangle$ is a multiscale interaction timescale for interphase TKE transfer first proposed by Pai and Subramaniam (2006). It was shown in Pai and Subramaniam (2006) that the new timescale accurately captures the dependence of the interphase TKE transfer on St_η. This timescale has been successfully employed in the context of EE two-phase turbulence modeling by Xu and Subramaniam (2006). The constant C_π is chosen to be 2.5 in this study. Details of the derivation relevant to the DLM timescale specification are reviewed here for the sake of completeness.

We first define a Stokes number valid in the inertial range as

$$St_l = \frac{\tau_{\text{p}}}{\tau_l}, \tag{22}$$

where τ_l is computed as

$$\tau_l = \frac{|\mathbf{u}_{\text{f}}|^2}{\varepsilon_{\text{f}}}. \tag{23}$$

Here, $\mathbf{u}_{\text{f}}$ is the exact Eulerian fluctuating velocity in the fluid phase. In order to derive the multiscale interaction timescale, the pdf of $|\mathbf{u}_{\text{f}}|$ is required. Using Eq. (3) the pdf of $\mathbf{u}$, which is a model for $\mathbf{u}_{\text{f}}$, can be computed directly from the solution. However, if the pdf of $\mathbf{u}$ remains joint normal during evolution, which is true for the test cases considered in this study (see Appendix B for details on the pdf of $\mathbf{u}_{\text{f}}$ implied by DLM), then one can derive an analytical form for the multiscale interaction timescale. Let $\mathbf{u}$ obey a joint normal distribution with zero mean and covariance $\sigma_{\text{f}}^2\delta_{ij}$, where $\sigma_{\text{f}}^2 = (2/3)k_{\text{f}}$ and δ_{ij} is the Kronecker delta. With this assumption, one can derive an expression for the pdf of $Z = |\mathbf{u}|$ as

$$f_Z(z) = \sqrt{\frac{2}{\pi}}\frac{1}{\sigma_{\text{f}}^3}z^2\exp(-z^2/2\sigma_{\text{f}}^2), \tag{24}$$

where z is the sample space variable corresponding to Z. A mean timescale of interaction $\langle\tau_{\text{int}}\rangle$ is derived from the pdf of $|\mathbf{u}|$ as

$$\langle\tau_{\text{int}}\rangle = \int_{|\mathbf{u}|^*}^{\infty}\tau_{\text{int}}f(z)\mathrm{d}z + \int_0^{|\mathbf{u}|^*}\tau_{\text{p}}f(z)\mathrm{d}z. \tag{25}$$

The timescale τ_{int} is hypothesized to be of the form

$$\tau_{\text{int}} = St_l(\tau_{\text{p}} - \tau) + \tau \tag{26}$$

for $|\mathbf{u}|^* \leqslant |\mathbf{u}| \leqslant \infty$. The significance of $|\mathbf{u}|^*$, and the rationale behind the choice of a weighted-average timescale $\langle\tau_{\text{int}}\rangle$ in Eq. (25), is now discussed.

Eq. (23) is based on an inertial sub-range scaling where eddies have a characteristic length scale l. The Stokes number St_l defined in Eq. (22) using the characteristic length scale determines how the droplets respond

to these eddies. For a value of $St_l > 1$, it is hypothesized that the droplet responds slowly to the eddies and the timescale of energy transfer is influenced more by the particle response time τ_p. On the other hand, if $St_l < 1$, it is hypothesized that the droplet responds immediately to the flow, and the timescale of energy transfer is influenced more by the eddy turnover timescale τ. Thus, the pdf of $|\mathbf{u}|$ (See Fig. 1) can be divided into two regions: one that represents $St_l > 1$, and the other that represents $St_l < 1$, with $|\mathbf{u}|^*$ representing the transition between the two regions at $St_l = 1$. Thus, $|\mathbf{u}|^*$ is uniquely determined by the relation $(|\mathbf{u}|^*)^2 = \tau_p \varepsilon_f$.

It is interesting to note that Eq. (25) has the correct behavior for limiting values of St_l and $|\mathbf{u}|^*$. In the limit $|\mathbf{u}|^* \to 0$, there are no eddies in the system with $St_l > 1$. The droplets are simply convected by the flow and the correct timescale for interphase TKE transfer in this limit is τ. In the limit $|\mathbf{u}|^* \to \infty$, practically all the eddies in the system satisfy $St_l > 1$, which implies that there are no eddies energetic enough to convect the droplets. The correct timescale for interphase TKE transfer in this limit is the particle response timescale τ_p.

For a polydispersed droplet size distribution, each droplet has a different τ_p. Since the timescale τ_{int} in Eq. (26) depends on, τ_p, each droplet can have a different interaction timescale τ_{int}. So, a multiscale interaction timescale $\langle \tau_{int} \rangle$ can be calculated for each droplet based on its particle response timescale. However, in the calculations presented in this work we use the mean value of τ_p computed from the polydispersed droplet ensemble, in place of τ_p, to compute τ_{int} in Eq. (26) to avoid prohibitively large computational run times.

Table 1 summarizes the model constants and timescales used in DLM.

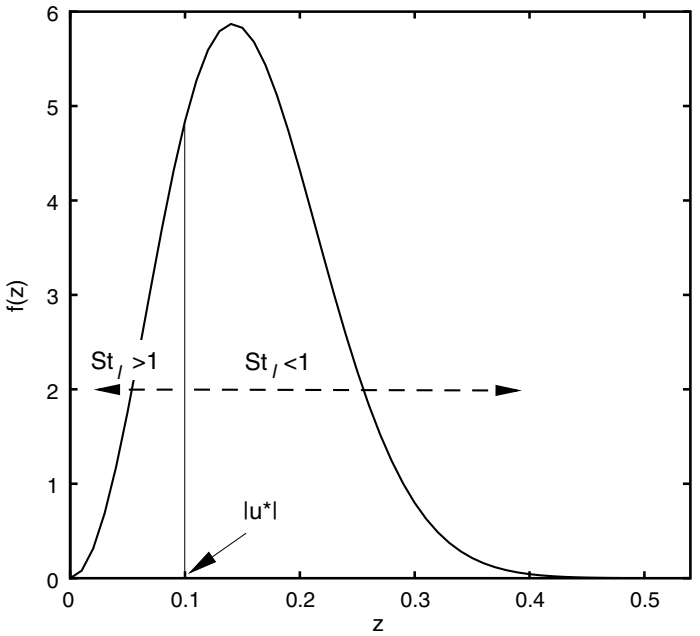

Fig. 1. A schematic probability density function of $|\mathbf{u}|$ that is used in the derivation of the multiscale interaction timescale $\langle \tau_{int} \rangle$. The sample space variable corresponding to $|\mathbf{u}|$ is z.

Table 1
Specification of model constants that appear in DLM for homogeneous particle-laden decaying and stationary turbulence

Model constant	Stationary case	Decaying case
C_k	$\frac{\phi(1-0.1St_\eta)}{1+\phi(1-0.1St_\eta)}$	Same
$1/\tau_1$	$C_1\phi/\tau$	Same
$1/\tau_2 = 1/\tau_4 = 1/\tau_\pi$	$C_\pi/\langle \tau_{int} \rangle$	Same
$1/\tau_3$	$2\left[\frac{1}{2\tau_1} + \left(\frac{3}{4}C_0\right)\frac{1}{\tau}\right]\frac{1}{1+St_\eta C_3}$	$2\left[\frac{1}{2\tau_1} + \left(\frac{1}{2}+\frac{3}{4}C_0\right)\frac{1}{\tau}\right]\frac{1}{1+St_\eta C_3}$

The constants $C_1 = 0.5$, $C_\pi = 2.5$ and $C_3 = 0.1$.

5. Test cases for model validation

Direct numerical simulations of non-evaporating and evaporating droplets in stationary turbulence have been performed by Mashayek et al. (1997). Simulation parameters used in the DNS are summarized in Table 2. We compare predictions from DLM against this DNS dataset since the DNS reports both TKE in each phase, and statistics related to droplet dispersion. In addition, since a simplified evaporating droplet regime is simulated, the behavior of DLM with temporally evolving droplet radii can be ascertained. The DNS (Mashayek et al., 1997) has been performed under the following assumptions:

Non-evaporating droplets:

(1) Droplets are in the sub-Kolmogorov size range.
(2) The point-particle approximation is employed to represent the droplets in the system.
(3) The droplets do not affect the fluid-phase momentum equation which implies that the simulations are one-way coupled.

Evaporating droplets:

In addition to the assumptions for non-evaporating droplets, the following assumptions hold for the evaporating droplets.

Spherically symmetric droplet vaporization is assumed, and constant-temperature droplets are assumed to vaporize in an infinite, isothermal gas phase. It is also assumed that the vaporizing droplets do not significantly alter the density of the surrounding gas, and all fluid-phase transport properties are assumed to be constant.

The d^2-law of vaporization is assumed wherein the rate of change of droplet surface area is a linear function of time (Faeth, 1977)

$$d_{\mathrm{p}}^2(t) = d_{\mathrm{p0}}^2 - \kappa t, \tag{27}$$

where $d_{\mathrm{p}}(t)$ is the droplet diameter at time t, d_{p0} is the droplet diameter at some initial time t_0 and κ is the evaporation rate given by relation (Faeth, 1977)

$$k = 8\Gamma_{\mathrm{f}} \ln(1 + B_M) C_{\mathrm{Re}}. \tag{28}$$

Here Γ_{f} is the fuel-vapor diffusivity coefficient (Lewis number of unity is assumed) and B_M is the Spalding transfer number. The correlation factor C_{Re} of the form

$$C_{\mathrm{Re}} = 1 + 0.3 Re_{\mathrm{d}}^{0.5} Sc_{\mathrm{d}}^{0.33} \tag{29}$$

proposed by Ranz and Marshall (1952) accounts for convective effects.

The droplet Reynolds number Re_{d} is defined as

$$Re_{\mathrm{d}} = \frac{|\mathbf{U}_{\mathrm{f}}(\mathbf{X}_{\mathrm{d}}, t) - \mathbf{V}_{\mathrm{d}}| d_{\mathrm{p}}}{\nu_{\mathrm{f}}}, \tag{30}$$

Table 2
Parameters used in the DNS (Mashayek et al., 1997)

Volume fraction θ	5.5×10^{-5}
Fluid-phase thermodynamic density ρ_f(kgm^{-3})	1.00
Dispersed-phase thermodynamic density ρ_d(kgm^{-3})	1000.00
Acceleration due to gravity g(ms^{-2})	0.0
Initial mean slip $\langle \mathbf{U}_f \rangle - \langle \mathbf{V}_d \rangle$(ms^{-1})	0.0,0.0,0.0
Turbulence intensity in fluid phase u'(ms^{-1})	0.019
Dissipation rate in fluid phase ϵ(m^{2}s^{-3})	3.98×10^{-6}
Kinematic viscosity of fluid ν(m^{2}s^{-1})	2.692×10^{-4}
Taylor scale Reynolds number Re_λ	41

where $\mathbf{U}_f$ is the gas-phase velocity at the location $\mathbf{X}_d$,$\mathbf{V}_d$ is the droplet velocity and $Sc_d = \nu_f/\Gamma_f$ is the droplet Schmidt number (Faeth, 1977). The evaporation constant κ varies in time only due to change in C_{Re}, which in turn depends on the temporal variation in Re_d.

Incorporating the d^2-law into the expression for the particle time constant defined as

$$\tau_p(t) = \frac{\rho_d}{\rho_f}\frac{d_p^2}{18\nu_f} \tag{31}$$

results in

$$\tau_p(t) = \tau_{p0} - \tau_e t, \tag{32}$$

where the initial particle time constant

$$\tau_{p0} = \frac{\rho_d}{\rho_f}\frac{d_{p0}^2}{18\nu_f}. \tag{33}$$

The non-dimensional quantity τ_e can be related to the momentum response time by

$$\tau_e = \frac{\rho_d\kappa}{\rho_f 18\nu_f} = \frac{\tau_p(t)\kappa}{d_p(t)^2} = \frac{\tau_p(t)}{\tau_{evap}}. \tag{34}$$

Thus, τ_e is the ratio of the mechanical response time of the particle to the remaining droplet lifetime $\tau_{evap} = d_p(t)^2/\kappa$, if the droplet evaporated at a constant vaporization rate from time t. A value of $\tau_e < 1$ implies that the time taken by the droplet to equilibrate with the flow is larger than the droplet lifetime. The ratio τ_e can be expressed in terms of C_{Re} as

$$\tau_e = C_{Re}\tau_{e0}, \tag{35}$$

where

$$\tau_{e0} = \frac{\rho_d}{\rho_f}\frac{4\Gamma_f}{9\nu_f}\ln(1+B_M) = \frac{\rho_d}{\rho_f}\frac{\kappa}{18\nu_f C_{Re}}. \tag{36}$$

Mashayek et al. (1997) report initial vaporization rates in terms of a parameter τ_{ec} that they relate to τ_{e0} by the relation

$$\tau_{e0} = 0.29\tau_{ec}/\tau. \tag{37}$$

More details on the parameter τ_{ec} and the reason for the coefficient 0.29 can be found in Mashayek et al. (1997). The initial evaporation rate is reported by specifying τ_{ec} in multiples of the Kolmogorov timescale τ_k. For a given value of τ_{ec}, τ_{e0} and κ are found using Eqs. (37) and (36), successively.

The non-evaporating test case is denoted **TNE**. Of the several test cases reported in the DNS with evaporating droplets, only three representative test cases are chosen in this work for the sake of brevity:

(1) Varying initial vaporization rates, constant initial particle response time, constant C_{Re} (**TE1**).
(2) Varying initial vaporization rates, varying initial particle response time, varying C_{Re} by changing Re_d, keeping $Sc_d = 1$ (**TE2**).
(3) Varying initial vaporization rates, varying initial particle response time, varying C_{Re} by changing both Re_d and Sc_d (**TE3**).

The other two cases analyzed in the DNS are (a) the effect of spray size and (b) the effect of initial drop size distribution. Since we restrict our study to a homogeneous evaporating spray, we do not analyze the effect of initial spray size. Additional terms including the change in mean velocity along, and transverse to, the axis of the spray need to be taken into account to study an inhomogeneous spray completely. Since such information is not reported in the DNS (Mashayek et al., 1997), we do not analyze this test case. Although the DLM is

capable of considering effects of initial spray size, for the sake of brevity, we do not analyze the test case involving varying drop size distributions. Also, drift effects due to gravity are not investigated in this study.

5.1. DLM in the limit of one-way coupling

If the mass loading $\phi \to 0$ in a two-phase flow system, then it is reasonable to assume one-way coupling. At the edges of an evolving spray, where the volume fraction of the liquid $\theta_d \ll 1$, the limit of one-way coupling could be achieved and it is important for a two-phase flow turbulence model to behave reasonably well in the one-way coupled limit. In this limit, the TKE in the fluid phase can be assumed to remain unaffected by the presence of the dispersed phase. Thus, terms representing interphase interaction in the evolution equation for the fluid-phase TKE Eq. (13) can be neglected.

An interesting feature of DLM is that, by virtue of the EoE hypothesis, it has the correct one-way coupled limiting behavior as the mass loading $\phi \to 0$. The interphase TKE transfer term in Eq. (8) turns out to be negligible in this limit. In other words, no additional treatment is necessary to introduce the physics governing the two-phase flow mixture in the one-way coupled limit into DLM. This observation can be explained as follows.

The specific equilibrium TKE in the fluid phase e_f^e defined in Eq. (16) can be rewritten as

$$k_f^e = (1 - C_k)\frac{\rho_m k_m}{\rho_f \theta_f} = (1 - C_k)(k_f + \phi k_d).$$

From Eq. (17), one can infer that for $\phi \to 0$ (limit of one-way coupling), $C_k = \phi k_d^e / k_f^e$ (since k_d^e / k_f^e is finite). This results in

$$\lim_{\phi \to 0} k_f^e = k_f,$$

which essentially implies that $\mathrm{d}k_f/\mathrm{d}t \sim 0$ in Eq. (8).

6. Model predictions

In this section, details of the numerical implementation and integration of the SDEs given by Eqs. (3) and (4) are first presented. Next, predictions from DLM are compared with DNS results for the test cases **TNE, TE1, TE2** and **TE3**. It is noted at the outset that we do not seek an exact match between predicted results and the DNS dataset used in model validation, rather we assess the capability of the new model in capturing trends of important two-phase flow statistics with varying Stokes number. A more detailed discussion is presented in Section 7.

6.1. Initialization of the computational ensemble

The fluid-phase turbulence simulated in the DNS (Mashayek et al., 1997) is isotropic at initial time, and owing to one-way coupling, remains isotropic in time. Corresponding to this initial condition, in DLM the initial velocity of a stochastic particle that represents the fluid phase is sampled from a joint normal distribution with zero mean and covariance matrix $(2/3)k_f\delta_{ij}$. In the DNS, the droplets are introduced into the fluid phase with the same velocity as the surrounding fluid. This fact affects the evolution of statistics like droplet Reynolds number that depend on velocities in both phases at the same position and time. However, since in DLM the particle Reynolds number calculation procedure (see next) randomly reorders the stochastic particles at every time step, it does not matter if particles with like indices across the phases have identical velocities at initial time or not. Nevertheless, we do ensure that $k_f(t = 0) = k_d(t = 0)$.

6.2. Computational details for the system of SDEs

An Euler–Maruyama (EM) scheme (Kloeden and Platen, 1992), which is the stochastic equivalent of the deterministic Euler scheme, is used to evolve the system of vector SDEs (cf. Eqs. (3) and (4)) in time. Since we are interested in mean quantities in this study, and because the weak order of convergence of the EM

scheme is unity (Kloeden and Platen, 1992), we choose this scheme to integrate the SDEs in time. Twenty multiple independent simulations (MIS) are performed for each case, and statistics are obtained by averaging over these MIS to reduce statistical error. The number of stochastic particles that represent each phase is the same, and equal to 10000. The statistical variability in the moments of the velocity, like TKE in the fluid phase k_f and dispersed phase k_d, and velocity autocorrelations in the both phases (cf. Eqs. (10) and (11)), across the 20 MIS is less than 3%. The time step required for accurate numerics is determined by performing a series of simulations with successively decreasing time steps. It is observed that for $\Delta t \leqslant 0.002 \min(\tau_p, \tau)$, the predicted moments did not change in a statistical sense. Therefore, this value of Δt is chosen for all the simulations. The runs for the evaporating cases are stopped when the minimum of the particle response times of all droplets is (1/20)th of the initial particle response time, in order to avoid prohibitively large computational times.

We estimate the droplet Reynolds number from the ensemble of stochastic particles in the following manner. The computational particles that represent the fluid phase are randomly paired with those that represent the dispersed phase at the beginning of each time step (note that the number of stochastic particles that represent each phase is the same). The Reynolds number estimate for the mth stochastic particle that represents the dispersed phase is computed as

$$Re_{d,(m)} = \frac{|\mathbf{u}_{(m)} - \mathbf{v}_{(m)}| d_{p,(m)}}{\nu_f}, \tag{38}$$

where $d_{p,(m)}$ is the diameter property associated with the mth stochastic particle. The mean droplet Reynolds number is calculated by averaging Eq. (38) over the stochastic particles that represent the dispersed phase as[5]

$$\langle Re_d \rangle = \frac{1}{N_p} \sum_{m=1}^{N_p} Re_{d,(m)}, \tag{39}$$

where $N_p = 10000$. We adopt this procedure to calculate $\langle Re_d \rangle$ since each stochastic particle represents only a realization of a stochastic process (cf. Eqs. (3) and (4)). Moreover, in the homogeneous ensemble of particles considered, each particle that represents the dispersed phase is equally likely to be next to a particle that represents the fluid phase.

6.3. Test case *TNE*

Mashayek et al. (1997) perform a test for stationarity in the non-evaporating case by reporting the evolution of the mean droplet Reynolds number $\langle Re_d \rangle$ (see Eq. (30) for the definition of Re_d). In the DNS, the angled brackets represent an averaging done over all droplets.

Predicted evolution of droplet Reynolds number for increasing Stokes number using DLM is shown in Fig. 2 against scaled time t/T_{ref}. Here $T_{ref} = l/u'$, where l is the Eulerian integral length scale and u' is the initial turbulence intensity in the fluid phase, both reported in the DNS (Mashayek et al., 1997).[6] From the figure it can be observed that the system reaches stationarity after $t/T_{ref} = 3.0$. As a result of the random pairing of particles to determine $\langle Re_d \rangle$, the initial evolution of $\langle Re_d \rangle$ does not start from zero as in the DNS. Although the trend with increasing Stokes number is predicted accurately, DLM overestimates the stationary value of $\langle Re_d \rangle$. To check whether this overestimation is a problem of numerical resolution, an analytical expression for $\langle Re_d \rangle$ as implied by DLM is derived in Appendix B where it is shown that the predictions from DLM are consistent with the analytical results (the analytical stationary value of $\langle Re_d \rangle$ is shown in Fig. 2 for each Stokes number).

Scaled equilibrium dispersed-phase TKE predicted by DLM is compared in Fig. 3 with results from DNS for increasing Stokes number. Since the turbulence in the fluid phase is forced to remain constant, the stationary TKE of the fluid phase is identical to the initial TKE $k_f(t_0)$. With decreasing Stokes number, the

[5] In inhomogeneous computations, the same procedure can be applied to the computational particles in each phase that occupy the same Eulerian grid cell.

[6] An alternative scaling of the time coordinate is the Eulerian integral timescale τ_E estimated by $(C_5/C_6)(u'^2/\varepsilon)$, where $C_5 = 0.212$ and $C_6 = 0.36$ (See Lu (1995), Hinze (1975)). It turns out that $\tau_E \sim T_{ref}$. However, the emphasis in this study is to match trends rather than seek an exact quantitative match with DNS results. Therefore, T_{ref} is retained as an appropriate scaling of the time co-ordinate.

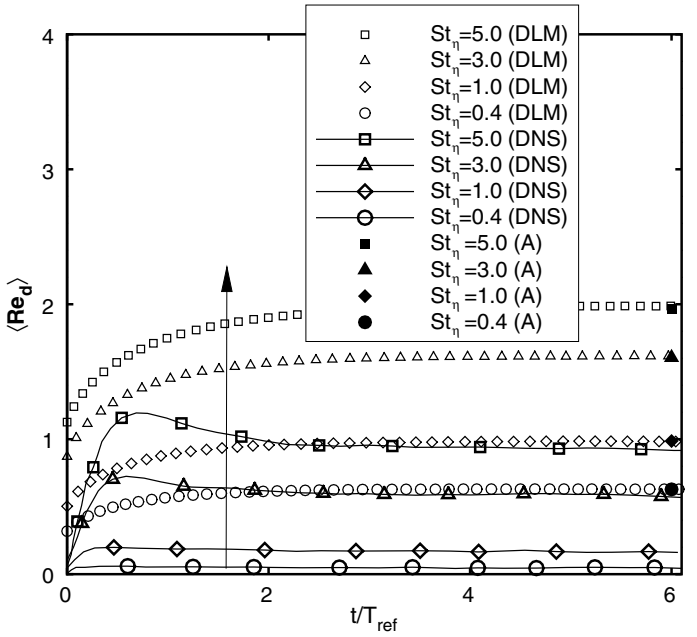

Fig. 2. Evolution of particle Reynolds number for the test case **TNE** (i) DLM; (ii) DNS results (Mashayek et al., 1997). Arrow indicates direction of increasing Stokes number. The letter '(A)' in the legend denotes analytical values computed using Eq. (B.4).

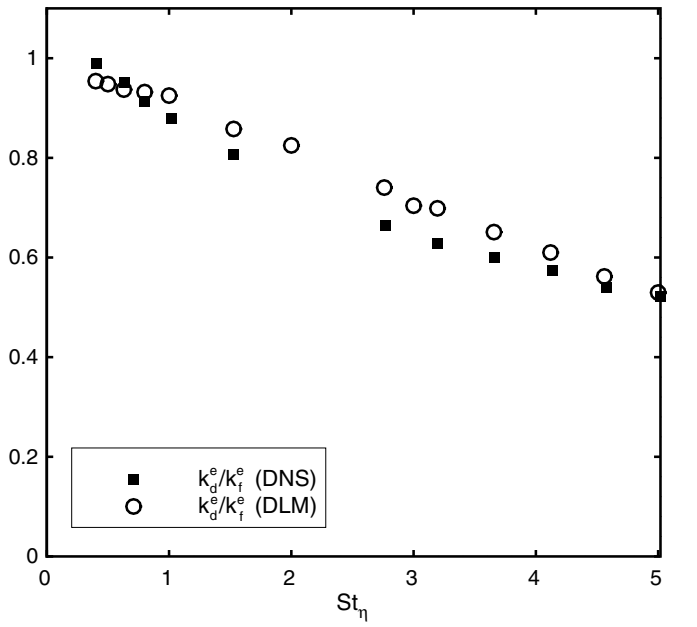

Fig. 3. Trend of equilibrium dispersed-phase turbulent kinetic energy k_d^e scaled by equilibrium fluid-phase turbulent kinetic energy k_f^e with increasing Stokes number St_η for the test case **TNE** (i) DLM (ii) DNS results (Mashayek et al., 1997).

equilibrium TKE in the dispersed phase should approach the equilibrium TKE in the fluid phase, a trend that is observed in the DNS. From the figure one can conclude that predictions of dispersed-phase equilibrium energies from DLM agree well with the DNS results.

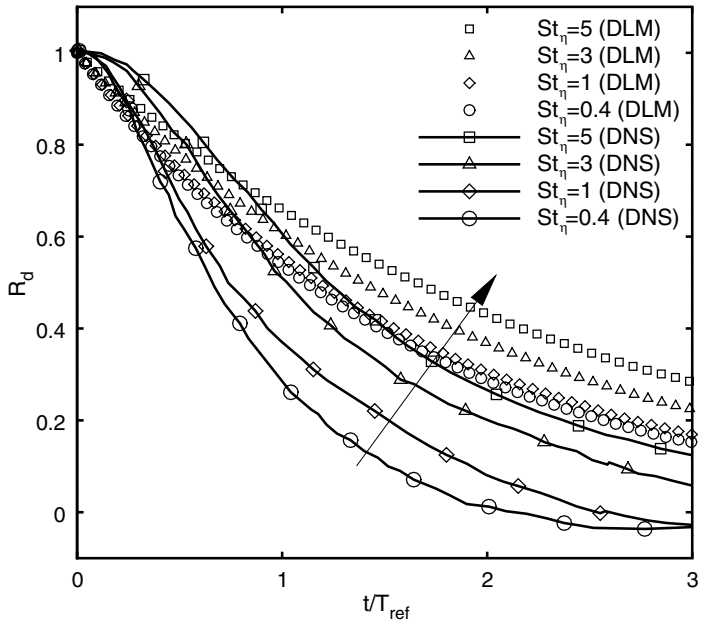

Fig. 4. Evolution of droplet-velocity autocorrelation R_d given by Eq. (9) for the test case **TNE** (i) DLM; (ii) DNS results (Mashayek et al., 1997). Arrow indicates direction of increasing Stokes number.

Predicted droplet-velocity autocorrelations from DLM using Eq. (9) are presented in Fig. 4 against scaled time t/T_{ref}. With increasing Stokes number, a droplet takes more time to lose correlation with its initial velocity resulting in larger timescales of droplet-velocity autocorrelation decay. Predicted trend in the autocorrelation decay with increasing Stokes number by DLM matches well with corresponding results from DNS.

Predictions from DLM for the asymptotic dispersed-phase diffusion coefficients $\alpha_d(\infty)$ computed using Eq. (12), scaled by the product of the initial turbulence intensity u' and the Eulerian integral length scale l, are reported in Fig. 5. Although DLM overestimates the asymptotic diffusion coefficient of the dispersed phase, the trend with increasing Stokes number matches DNS results. Also, shown on the same figure is the fluid-phase asymptotic diffusion coefficient $\alpha_f(\infty)$ computed using DLM. As predicted by theoretical calculations (See G. Gouesbet and Picart (1984) for a discussion on Tchen's analysis (Tchen, 1947)), the dispersed-phase asymptotic diffusion coefficient matches with that of the fluid-phase as $St_\eta \to 0$. Again, to see if the overestimation of $\alpha_d(\infty)$ is a problem of numerical resolution, an analytical estimate of the asymptotic diffusion coefficient as implied by DLM is given in Appendix C. It is seen that DLM predictions are consistent with the analytical estimates.

6.4. Test case *TE1*

In this test case, the radii of initially monodispersed droplets evolve according to the d^2-law given by Eq. (27). All droplets evolve by a constant vaporization rate such that each droplet's radius reduces by the same amount in time. This is accomplished by assuming that C_{Re} remains at unity (or $Sc_d = 0$, which implies infinitely fast diffusion of the fuel vapor in the gas). The initial particle response time is the same across all the runs. As the droplet radii decrease in time their Stokes numbers St_η decrease and the droplets respond faster to the flow disturbances, thereby losing correlation with their initial velocity faster. Thus, when vaporization is included, droplet-velocity autocorrelations decay faster compared to the case with no evaporation ($\tau_{ec} = 0$). The faster decay in autocorrelations is accentuated at higher initial vaporization rates.

Predicted evolution of droplet-velocity autocorrelations for different initial vaporization rates and for an initial particle time constant $\tau_{p0} = 5\tau_\eta$ (i.e. $St_\eta = 5$) using DLM is shown in Fig. 6. DLM shows a reasonable match with the autocorrelations from DNS and also matches the trend with increasing vaporization rate.

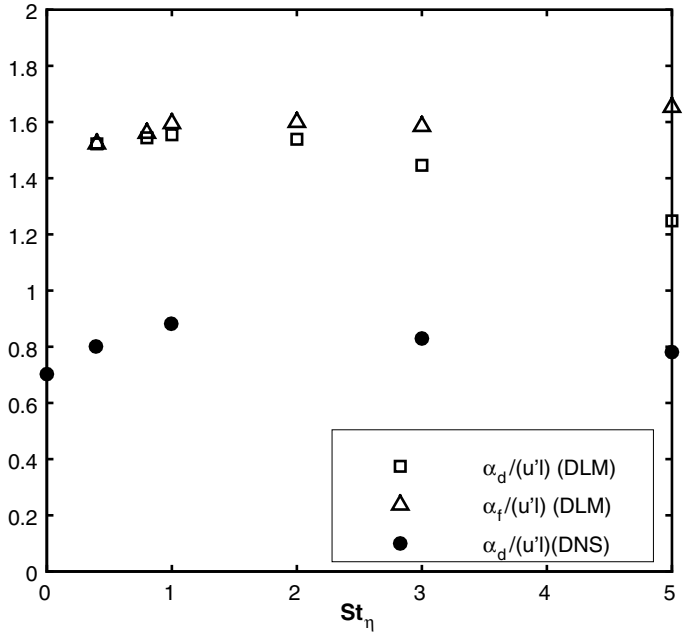

Fig. 5. Trend of asymptotic diffusion coefficient $\alpha_d(\infty)$ in the dispersed phase with increasing Stokes number St_η for the test case **TNE** (i) DLM; (ii) DNS results (Mashayek et al., 1997). Also shown is the trend of asymptotic fluid-phase diffusion coefficient $\alpha_f(\infty)$ as predicted by DLM for this range of Stokes numbers.

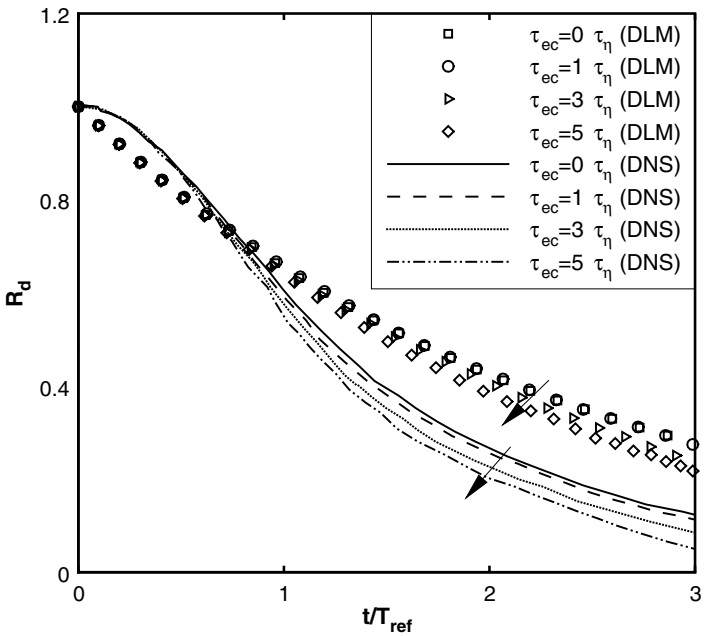

Fig. 6. Evolution of droplet-velocity autocorrelation R_d given by Eq. (9) for a constant initial Stokes number $St_\eta = 5.0$ and varying vaporization rates for test case **TE1** (i) DLM; (ii) DNS results (Mashayek et al., 1997). Arrow indicates direction of increasing initial vaporization rate.

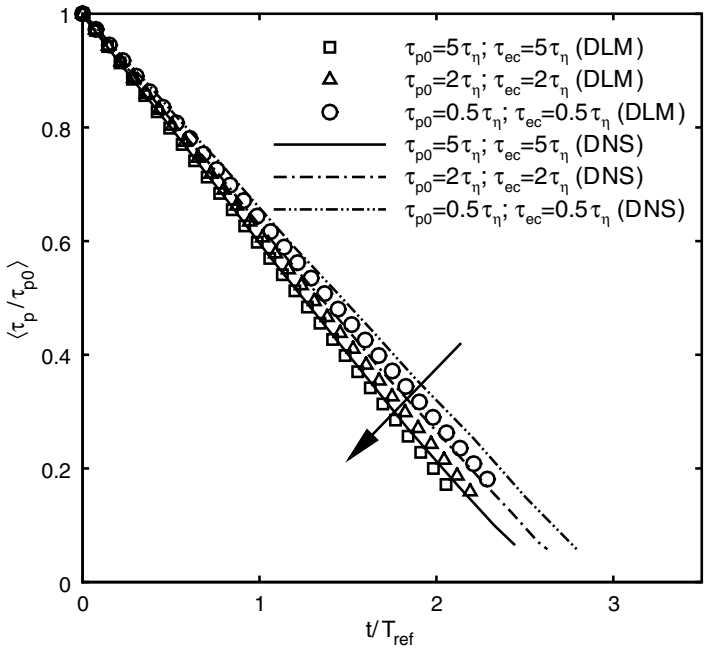

Fig. 7. Predicted trend of scaled particle response time for varying initial vaporization rates and varying initial particle response time for for the test case **TE2** (i) DLM (ii) DNS results (Mashayek et al., 1997). Arrow indicates direction of increasing initial Stokes number St_η and initial vaporization rate.

6.5. Test case *TE2*

Droplet vaporization rates, which were constant in time for each droplet in test case **TE1**, are allowed to change in this test case by allowing for a non-zero Sc_d (in this case $Sc_d = 1$). The dependence of vaporization rate on Re_d through the assumed correlation Eq. (29) results in a radius evolution that is different for each droplet. Consequently, an initially monodispersed ensemble of droplets becomes polydispersed in time. Evolution of particle response time normalized by its initial value averaged over all the particles is shown in Fig. 7. A linear decay in the scaled particle response time is observed in DLM which is consistent with the DNS results.

The d^2-law predicts that, for constant vaporization rate κ, droplets with smaller radii evaporate faster than ones with larger radii. Since κ depends on Re_d through the correlation for C_{Re} in Eq. (29), each droplet has different initial vaporization rates at initial time due to different droplet Reynolds numbers arising from the initial distribution of droplet velocities (cf. Eq. (30)). As d_p decreases, Re_d decreases which slows down the vaporization rate. Once a droplet starts to evaporate, a competition between the d^2-law and the vaporization rate is observed. The DNS predicts that the standardized pdf of d_p becomes more Gaussian as τ_p increases. A negative value of skewness in the standardized pdf of d_p is expected, since owing to the d^2-law, the probability of finding large particles in the computational domain is higher than finding smaller ones at long time.[7] From Fig. 8 one can infer that in the DNS the skewness of the standardized pdf of d_p remains largely on the negative side, becoming more negative towards the end. Also, the DNS shows that the kurtosis is closer to Gaussian, especially in between $t/T_{ref} = 1$ and $t/T_{ref} = 2$.

Skewness and kurtosis predictions from DLM are shown in Fig. 8. DLM predicts a larger particle Reynolds number compared to the DNS (see Fig. 2 for the stationary case), thereby overestimating the vaporization

[7] The skewness and kurtosis of the standardized pdf of the particle diameter d_p characterizes the polydispersity of the spray droplets. Skewness measures the degree of asymmetry of a distribution (Abramowitz and Stegun, 1964). Skewness for a Gaussian random variable is 0. The kurtosis characterizes the peakedness of the distribution. Kurtosis for a Gaussian random variable is 3.

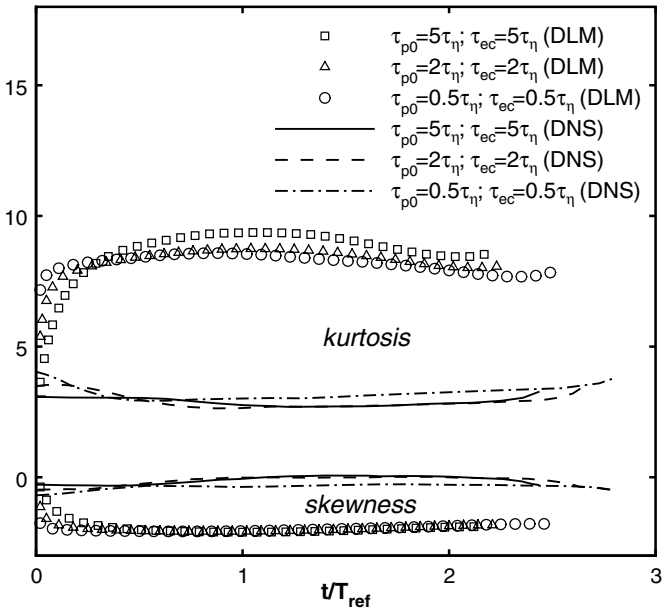

Fig. 8. Evolution of skewness and kurtosis of droplet diameter d_p for varying initial vaporization rates and varying initial particle response time for the test case **TE2** (i) DLM; (ii) DNS results (Mashayek et al., 1997).

rate. This results in a larger negative skewness compared to the DNS results. The effect of an overestimated vaporization rate is also seen in the kurtosis predicted by DLM showing a value much larger than 3. This implies that the pdf of d_p predicted by DLM is more peaked than that seen in the DNS. However, the approximate flattening of the kurtosis in between $t/T_{ref} = 0.5$ and $t/T_{ref} = 1.5$ illustrates that DLM does capture the competing effects of vaporization rate and the d^2-law as the droplets evolve. DLM predicts a trend of an increasing kurtosis and decreasing skewness towards the end of the simulation, similar to that seen in DNS, although the trends are more pronounced in the DLM predictions. Droplets with smaller initial vaporization rate and Stokes number tend to remain longer in the DNS, a trend that is captured by DLM. A comparison of the pdf of $\tau_p^{(1/2)}$ (or d_p) for initial $St_\eta = 5$ and $\tau_{ec} = 5\tau_\eta$ with that from the DNS results is shown in Fig. 9 for different scaled times.[8] As suggested by the higher (positive) kurtosis and a negative skewness of $\tau_p^{1/2}$ from DLM (cf. Fig. 8) compared to the DNS, the pdf of $\tau_p^{1/2}$ is more peaked with longer left tails than the corresponding DNS results.

6.6. Test case *TE3*

The effect of changing Sc_d for different initial vaporization rates and particle response times is now considered. Mashayek et al. (1997) present two sets of results in this test case depending on how the simulation is initialized: in the first case, the relative velocity between the droplets and the surrounding fluid is zero (non-stationary initial state) and in the second case, the initial state of the droplet-laden turbulent flow is stationary. The value of $\langle C_{Re} - 1\rangle$ is tracked in these cases which for a constant Sc_d measures how $\langle Re_d^{1/2}\rangle$ (cf. Eq. (29)) evolves in time.

For the non-stationary initial state, the droplet Reynolds number at initial time is zero in the DNS. Once the droplets start to evolve the Reynolds number increases due to a finite relative velocity. At the same time, the droplet diameter is decreasing due to vaporization. A maximum value in the evolution of Reynolds number is reached, analogous to that seen in case **TNE** (see Fig. 2). In time, the effect of the decreasing diameter

[8] The exact scaling of the ordinate for the pdf plot reported in the DNS is not clear, since the pdf from the DNS does not appear to integrate to unity. So we make a qualitative comparison of the pdf of $\tau_p^{(1/2)}$ from DLM with that from the DNS on the same plot with different ordinates.

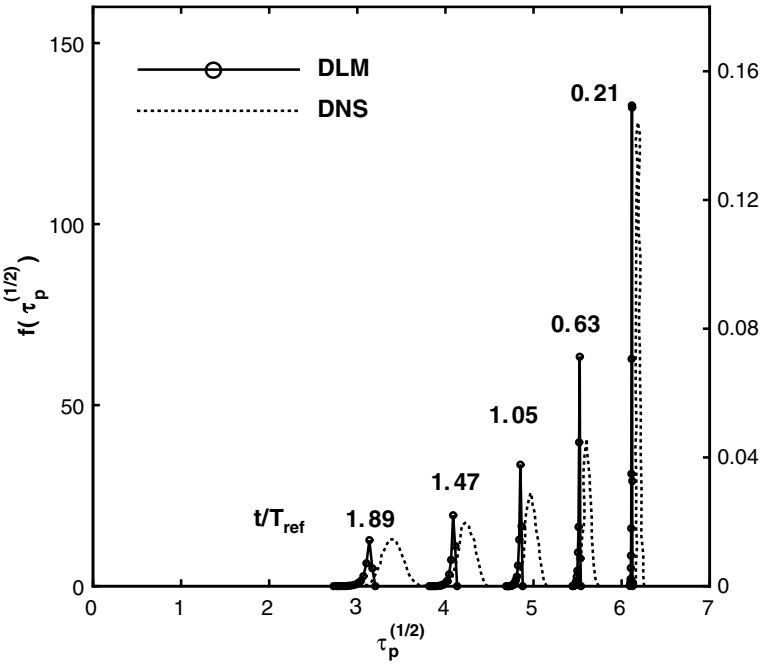

Fig. 9. Predicted evolution of the probability density function of $\tau_p^{1/2}$ for $St_\eta = 5, \tau_{ec} = 5\tau_\eta$ and $Sc_d = 1$ for the test case **TE2** (i) DLM; (ii) DNS results (Mashayek et al., 1997). The right-hand side ordinate is taken from the DNS results while the left-hand side ordinate is from DLM.

offsets the increase in the relative velocity and the particle Reynolds number starts to decrease. As is evident from the DNS results presented in Figs. 10 and 11 for initial Stokes numbers $St_\eta = 0.5$ and 5, respectively, increasing Sc_d increases the rate of evolution of $\langle C_{Re} - 1 \rangle$ although the maximum is reached at almost the same scaled time.

Fig. 10 shows the predicted trend in the evolution of $\langle C_{Re} - 1 \rangle$ by DLM for $St_\eta = 0.5$. As observed in the non-evaporating case, the droplet Reynolds number is overestimated by DLM in this case. This results in an overestimate of $\langle C_{Re} - 1 \rangle$. Again as a result of the random pairing of particles to determine $\langle Re_d \rangle$ in DLM, $\langle C_{Re} - 1 \rangle$ does not start from zero as in the DNS. However, the trend with increasing Sc_d is identical to that seen in the DNS. The same behavior is seen in the predicted trends of $\langle C_{Re} - 1 \rangle$ for initial $St_\eta = 5$ in Fig. 11.

For the stationary initial condition and a value of $Sc_d = 1$, the droplets have a attained stationary mean Reynolds number and the flow has reached a stationary state prior to the start of vaporization. Once vaporization is initiated, the particle Reynolds number begins to decrease due to a decrease in the diameter. Fig. 12 shows that the predicted trend for the two initial particle response times from DLM matches with DNS results.

6.7. Interphase mass transfer terms in the dispersed-phase TKE evolution equation

With no interphase mass transfer, as in the test case **TNE**, the only term that governs the evolution of the dispersed-phase TKE is the interphase TKE transfer term $\widetilde{\langle A_i v_i'' \rangle}$ (cf. Eq. (A.5) in the Appendix). However, in the presence of interphase mass transfer, as in the test cases **TE1-TE3**, additional terms appear in the evolution equation for the dispersed-phase TKE. These additional terms, namely, $3n\langle R^3 \rangle \widetilde{\langle v_i'' v_i'' \Gamma | t \rangle}$ and $6n\langle R^3 \rangle \tilde{k}_d \langle \tilde{\Gamma} | t \rangle$ in Eq. (A.5) in the Appendix, represent the contribution to the dispersed-phase TKE due to interphase mass transfer. It has to be borne in mind that two-phase models may give correct predictions for the dispersed-phase TKE in flows with mass transfer even if the individual contributions in the TKE evolution equation (cf. Eq. (A.5)) are not accurately modeled. DNS of evaporating two-phase flows possess the capability to quantify these terms. However, to our knowledge the DNS datasets available in the literature do not report

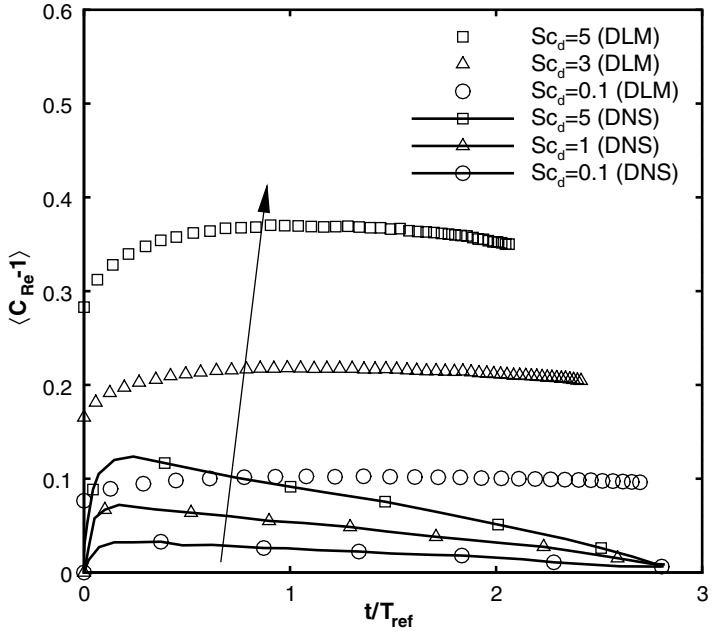

Fig. 10. Predicted trend of $\langle C_{\mathrm{Re}} - 1\rangle$ for varying Sc_{d} and $\tau_{\mathrm{p0}} = 0.5\tau_{\mathrm{k}}, \tau_{\mathrm{ec}} = 0.5\tau_{\mathrm{k}}$ evolving from a non-stationary initial state, for **TE3** (i) DLM; (ii) DNS (Mashayek et al., 1997). Arrow shows direction of increasing Sc_{d}.

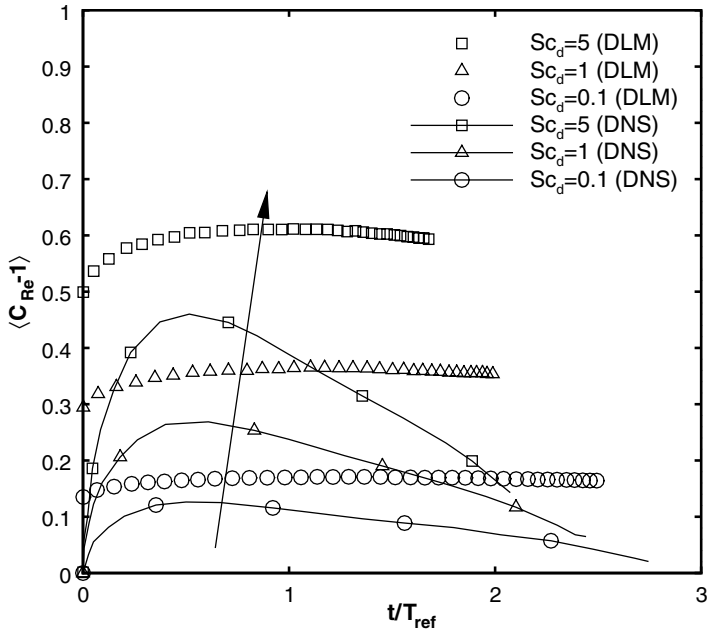

Fig. 11. Predicted trend of $\langle C_{\mathrm{Re}} - 1\rangle$ for varying Sc_{d} and $\tau_{\mathrm{p0}} = 5\tau_{\mathrm{k}}$, $\tau_{\mathrm{ec}} = 5\tau_{\mathrm{k}}$ evolving from a non-stationary initial state, for **TE3** (i) DLM (ii) DNS (Mashayek et al., 1997). Arrow shows direction of increasing Sc_{d}.

budgets of the interphase mass transfer terms. Therefore, we do not quantify these terms from DLM since we do not have any datasets to compare with. If available, model predictions of these individual terms can be compared with DNS data, thereby resulting in a more rigorous validation of any two-phase flow turbulence model.

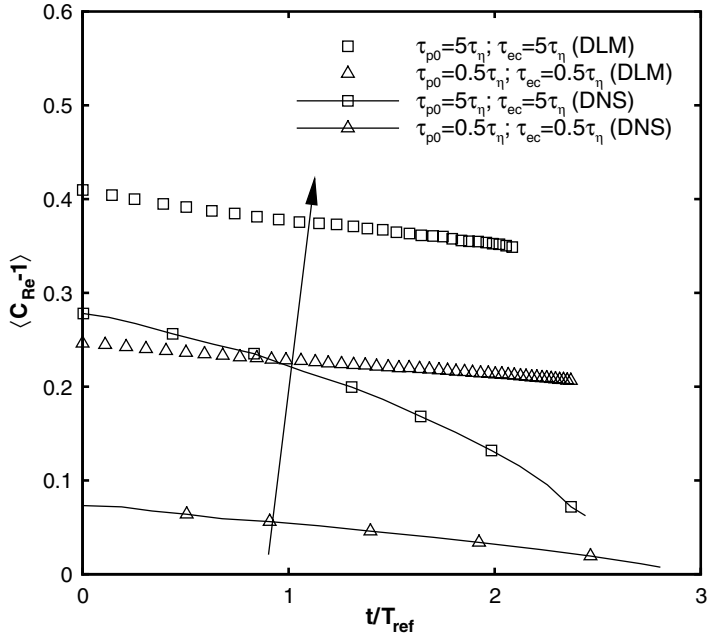

Fig. 12. Predicted trend of $\langle C_{\mathrm{Re}} - 1\rangle$ for $Sc_{\mathrm{d}} = 1$ with two initial values of particle response time and vaporization rates, evolving from a stationary initial state, for **TE3** (i) DLM, (ii) DNS (Mashayek et al., 1997). Arrow shows direction of increasing initial Stokes number St_η.

7. Discussion

In all the test cases presented above, it is clear that DLM captures the correct trend in the evolution of certain key statistics related to both non-evaporating and evaporating droplet-laden two-phase turbulent flow. It is fair to conclude that even though DLM has been derived taking two-way coupling into consideration, it has performed reasonably well in predicting droplet dispersion characteristics and TKE in the limit of one-way coupled droplet-laden turbulence.

The one-way coupled case considered is a simplified test case, applicable only in certain dilute spray regimes. Nevertheless, the one-way coupled limiting behavior of a two-phase flow turbulence model can be analyzed and also the behavior of certain important model constants can be ascertained through this comparison.

The reasons for the emphasis in this study on predicting only the trends correctly rather than seeking an exact quantitative match are manifold. In DNS of particle-laden flow (Sundaram and Collins, 1999; Mashayek et al., 1997; Squires and Eaton, 1991), although the gas phase is treated accurately by solving the full Navier–Stokes equations, the no-slip condition on the surface of each particle is not enforced. Also, since the flow around each particle is not resolved, a drag model of the form derived by Maxey and Riley (1983) is used to evolve particle velocities in time. The influence of the particle on the fluid-phase momentum equation is included by means of a modeled source term. It is important to recognize that the point–particle assumption for the *particle drag* in such DNS is justified in a limited flow regime where particle Reynolds numbers Re_{d} are $\mathcal{O}(1)$, dispersed phase to fluid density ratios $\rho_{\mathrm{d}}/\rho_{\mathrm{f}}$ are $\mathcal{O}(1000)$, and particles are sub-Kolmogorov size with negligible wake effects. The homogeneous problem that forms the basis of the investigation in this work and for which DNS datasets exist corresponds to a flow regime where the assumptions mentioned earlier are valid.

However, volume-displacement effects are neglected in such DNS and the carrier-phase velocity field is assumed to be solenoidal. Also, particle–particle (or drop–drop) interaction effects are not accounted for in such DNS, and the effect of the point–particle approximation on the true pressure field is also not quantified. The only way to test whether these approximations are justified is to perform *true* DNS where the flow around each droplet is fully resolved and exact boundary conditions are imposed on each droplet surface. The

assumption of solenoidality of the gas-phase velocity (which in turn affects the fluid pressure field), and neglect of droplet–droplet interaction effects, can only be tested in a true DNS. Recent studies by Ten Cate et al. (2004) are emerging which seek to assess the consequences of the point–particle approximation. They perform fully resolved simulations of particle-laden stationary turbulence in the same particle Stokes number and particle mass loading range as in the DNS study by Boivin et al. (1998) which uses a point–particle approximation for the dispersed phase. Ten Cate et al. (2004) find that the decrease in the rate of energy dissipation at the large scales is of the same order as that found by Boivin et al. (1998). However, one should note that the particle diameter is smaller than the Kolmogorov length scale, particle to fluid density ratios are $\mathcal{O}(1000)$ and the particle Reynolds numbers are $\mathcal{O}(1)$ in the DNS performed by Boivin et al. (1998). On the other hand, the particle diameters are larger than the Kolmogorov length scale, particle to fluid density ratios are $\mathcal{O}(1)$ and particle Reynolds numbers are $\mathcal{O}(10)$ in the fully resolved DNS performed by Ten Cate et al. (2004) and their simulations do not fall in the regime of two-phase flows investigated in this study.

Therefore, the DNS datasets performed with the point–particle approximation that are used in this study are the best data available for model testing and validation. It appears very likely that the existing DNS datasets *do* capture the major trends of the TKE variation and autocorrelation evolution with important non-dimensional parameters like Stokes number and mass loading. It is possible that true DNS such as the one performed by Ten Cate et al. (2004) might lead to revision in the exact quantitative predictions. Owing to all the reasons cited above, our principal conclusions concern qualitative trends predicted by DLM, rather than an exact quantitative match with available DNS data.

8. Conclusions

Direct numerical simulations of particle-laden flow confirm the existence of two disparate timescales, one governing particle dispersion and the other governing the interphase TKE transfer, that behave differently with Stokes number. In this context, the principal conclusions and achievements of this study are:

(1) Two-phase flow turbulence models should possess the capability to capture these disparate timescales observed in simple two-phase flow DNS. They should also possess the capability to capture the trends of these timescales with varying Stokes number in these simple flow configurations in order to be predictive in more complex spray computations.
(2) A new dual-timescale Langevin Model, based on the Equilibration of Energy concept is proposed. A novel feature of the proposed model is the incorporation of dual timescales, which can be specified to match the disparate trends in the evolution of TKE and velocity autocorrelation with varying Stokes number and mass loading.
(3) DLM predicts correct trends in stationary dispersed-phase TKE, dispersed-phase velocity autocorrelation decay and asymptotic droplet diffusion coefficients in droplet-laden stationary turbulence for a range of Stokes numbers.
(4) In the evaporating-droplet test case, DLM predicts pdf and moments of the droplet diameter that are in reasonable agreement with DNS results. Thus, DLM performs well in the simplified evaporating droplet regime accessed by the DNS.

Important terms in the evolution equation of the dispersed-phase TKE are identified in both the LE and EE statistical representations of two-phase flow. This exercise can serve as a guiding framework for generating datasets from future DNS of evaporating droplet-laden flow that are helpful to the two-phase flow modeling community.

Acknowledgement

This work is partially supported by a US Department of Energy, Early Career Principal Investigator Program Grant No. DE-FG02-03ER25550.

Appendix A. Exact equations for the dispersed-phase velocity covariance in a two-phase flow

The evolution equation for the dispersed-phase velocity covariance derived using the Lagrangian–Eulerian (LE) representation is presented here. The primary objective of this section is to identify unclosed terms in the equation that need to be modeled. The connection between DLM and the LE approach will also be explained here.

The governing equations for the dispersed phase in the LE representation are derived using the spray equation, which is the evolution equation for the droplet distribution function (ddf). First proposed by Williams (1958), the droplet distribution function $f(\mathbf{x},\mathbf{v},r,t)$ gives the probable number of droplets with positions in the range $\mathbf{x}+\mathrm{d}\mathbf{x}$, velocities in the range $\mathbf{v}+\mathrm{d}\mathbf{v}$ and radii in the range $r+\mathrm{d}r$. The phase space may also include other quantities like droplet temperature, droplet distortion from sphericity and rate of change of distortion from sphericity (See Amsden et al. (1989), for example). The theoretical foundations of the LE approach have been established by Subramaniam (2001, 2000), who has shown that the ddf can be decomposed into a conditional joint pdf of velocity and radius $f^c_{\mathbf{V}R}(\mathbf{v},r|\mathbf{x};t)$, and drop number density $n(\mathbf{x};t)$ as

$$f(\mathbf{x},\mathbf{v},r,t)=f^c_{\mathbf{V}R}(\mathbf{v},r|\mathbf{x};t)n(\mathbf{x};t).$$

Subramaniam (2001) has also shown that the ddf can be related to the single surrogate-droplet density $f^{(m)}_{1s}(\mathbf{x},\mathbf{v},r;t)$ as

$$f(\mathbf{x},\mathbf{v},r,t)=\sum_{m\geqslant 1}p_m m f^{(m)}_{1s}(\mathbf{x},\mathbf{v},r;t), \tag{A.1}$$

where p_m is the probability that the number of droplets in the system at any time t is equal to m.

The single surrogate droplet-density is the density of identically distributed surrogate droplets in phase space. This density has important implications in particle method solutions, like the one used in this study, of the spray equation where each *computational* particle is assumed to be an identically distributed realization of the spray. The Lagrangian joint probability density function of velocity and radius implied by a stochastic model like DLM can be identified with $f^{(m)}_{1s}$, and hence every model for the particle velocity in turn implies a modeled spray equation.

In order to derive an equation for the dispersed-phase velocity covariance, we define a volume-weighted or r^3-weighted[9] ddf of fluctuating velocity $\tilde{g}(\mathbf{x},\mathbf{w},r,t)$ as (Subramaniam, 2003; Pai and Subramaniam, 2006).

$$\tilde{g}(\mathbf{x},\mathbf{w},\mathbf{r},t)=\langle R^3(\mathbf{x};t)\rangle n(\mathbf{x};t)\tilde{f}^c_{\mathbf{V}R}\big(\langle\tilde{\mathbf{V}}|\mathbf{x};t\rangle+\mathbf{w},r|\mathbf{x};t\big), \tag{A.2}$$

where $\tilde{f}^c_{\mathbf{V}R}=(r^3/\langle R^3\rangle)f^c_{\mathbf{V}R}$. The fluctuating velocity in the dispersed-phase $\mathbf{w}$ is defined as

$$\mathbf{w}=\mathbf{v}-\langle\tilde{\mathbf{V}}|\mathbf{x};t\rangle,$$

where $\langle\tilde{\mathbf{V}}|\mathbf{x};t\rangle$ is the r^3–weighted mean of the dispersed-phase velocity and $\mathbf{v}$ is the sample space variable for the instantaneous velocity.

Under conditions of statistical homogeneity, the dependence of $\tilde{g}$ on $\mathbf{x}$ can be neglected and the evolution equation for $\tilde{g}$ simplifies to (Subramaniam, 2003; Pai and Subramaniam, 2006)

$$\frac{\partial\tilde{g}}{\partial t}=-\frac{\partial}{\partial w_{\mathrm{k}}}(\langle A_k|\mathbf{v},r;t\rangle\tilde{g})-\frac{\partial}{\partial r}(\langle\Theta|\mathbf{v},r;t\rangle\tilde{g})+3\langle\Gamma|\mathbf{v},r;t\rangle\tilde{g}, \tag{A.3}$$

[9] Volume-weighted averages of any smooth function $Q(\mathbf{v},r)$ are defined as

$$\langle\tilde{Q}\rangle\equiv\frac{\langle R^3Q\rangle}{\langle R^3\rangle}=\frac{\int_{[\mathbf{v},r_+]}r^3Qf^c_{\mathbf{V}R}(\mathbf{v},r|\mathbf{x};t)\mathrm{d}\mathbf{v}\ \mathrm{d}r}{\int_{[\mathbf{v},r_+]}r^3f^c_{\mathbf{V}R}(\mathbf{v},r|\mathbf{x};t)\mathrm{d}\mathbf{v}\mathrm{d}r},$$

where r_+ denotes the region $0\leqslant r<\infty$, while the number-weighted average of any smooth function $Q(\mathbf{v},r)$ is defined as

$$\langle Q\rangle=\int_{[\mathbf{v},r_+]}Qf^c_{\mathbf{V}R}(\mathbf{v},r|\mathbf{x};t)\mathrm{d}\mathbf{v}\mathrm{d}r,$$

and for the special case of monodisperse particles $\langle\widetilde{Q}\rangle=\langle Q\rangle$.

where $\langle A_k|\mathbf{v},r;t\rangle$ represents the expected acceleration (rate of change of velocity) conditional on location $[\mathbf{v},r]$ in phase space, $\langle \Theta|\mathbf{v},r;t\rangle$ represents the expected rate of change of radius conditional on $[\mathbf{v},r]$ and

$$\langle \Gamma|\mathbf{v};t\rangle = \left\langle \frac{\Theta}{R}\middle|\mathbf{v};t\right\rangle,$$

which is the vaporization rate scaled by radius. A more detailed discussion on these terms and their derivation can be found in Subramaniam (2001, 2000).

From Eq. (A.3), the evolution equation for the covariance of the dispersed phase velocity (assuming homogeneity) can be derived as (Subramaniam, 2003; Pai and Subramaniam, 2006)

$$n\langle R^3\rangle\left(\frac{\partial}{\partial t}\widetilde{\langle v_i'' v_j''\rangle}\right) = n\langle R^3\rangle\left(\widetilde{\langle A_i v_j''\rangle} + \widetilde{\langle A_j v_i''\rangle}\right) + 3n\langle R^3\rangle\langle\widetilde{v_i'' v_j''\Gamma}|t\rangle - 3n\langle R^3\rangle\widetilde{\langle v_i'' v_j''\rangle}\langle\tilde{\Gamma}|t\rangle \tag{A.4}$$

where

$$\widetilde{\langle v_i'' v_j''\rangle} \equiv \int_{[\mathbf{v},r_+]} w_i w_j \tilde{f}^c_{\mathbf{V}R}(\langle\tilde{\mathbf{V}}|\mathbf{x};t\rangle + \mathbf{w}, r|\mathbf{x};t)\,\mathrm{d}\mathbf{w}\,\mathrm{d}r.$$

The first term on the right-hand side of Eq. (A.4) is the acceleration-fluctuating velocity correlation

$$n\langle R^3\rangle\left(\widetilde{\langle A_i v_j''\rangle} + \widetilde{\langle A_j v_i''\rangle}\right),$$

while the remaining two terms can be grouped together to represent the net velocity covariance change due to interphase mass transfer

$$+3n\langle R^3\rangle\langle\widetilde{v_i'' v_j''\Gamma}|t\rangle - 3n\langle R^3\rangle\widetilde{\langle v_i'' v_j''\rangle}\langle\tilde{\Gamma}|t\rangle.$$

Models for particle velocity and droplet vaporization in turn imply models for $\langle A_i\rangle$ and $\langle\Theta\rangle$. In particle-based LE approaches like DLM (also Amsden et al. (1989)), the terms on the right-hand side of Eq. (A.4) are closed and can be determined from the solution.

Contracting indices in Eq. (A.4) results in an evolution equation for the r^3-weighted TKE in the dispersed phase $\tilde{k}_\mathrm{d} = (1/2)\widetilde{\langle v_i'' v_i''\rangle}$ as

$$2n\langle R^3\rangle\frac{\partial}{\partial t}\tilde{k}_\mathrm{d} = 2\langle R^3\rangle n\widetilde{\langle A_i v_i''\rangle} + 3n\langle R^3\rangle\langle\widetilde{v_i'' v_i''\Gamma}|t\rangle - 6n\langle R^3\rangle\tilde{k}_\mathrm{d}\langle\tilde{\Gamma}|t\rangle. \tag{A.5}$$

With no interphase mass transfer, as in non-evaporating or solid particle-laden turbulent flow, and monodispersed particles, the terms involving Γ are zero. Also, volume-weighted quantities are the same as their number-weighted counterparts. The above equation then simplifies to

$$\frac{\partial}{\partial t}k_\mathrm{d} = \langle A_i v_i''\rangle.$$

Thus, in a homogeneous two-phase flow with *no interphase mass transfer* the evolution of the dispersed-phase TKE is governed only by the acceleration-fluctuating velocity covariance.

A.1. Correspondence with the Eulerian–Eulerian statistical representation of two-phase flows

For a homogeneous two-phase flow, there is a correspondence between the governing equations for the dispersed-phase TKE derived using the LE and Eulerian–Eulerian (EE) representation of two-phase flow. This correspondence allows one to estimate an unclosed term on the EE side using the corresponding term on the LE side.

Under assumptions of statistical homogeneity, one can derive the evolution equation for the density-weighted dispersed-phase TKE, defined as

$$\tilde{k}_\mathrm{d} = \langle I_\mathrm{d}\rho u_{\mathrm{d}_i}'' u_{\mathrm{d}_i}''\rangle/\langle I_\mathrm{d}\rho\rangle, \tag{A.6}$$

in the EE representation as (Drew, 1983; Subramaniam, 2003; Xu, 2004) as

$$\theta_d \rho_{\mathrm{d}} \frac{\mathrm{d}}{\mathrm{d}t}\tilde{k}_{\mathrm{d}} = \left\langle u''_{\mathrm{d}_i} \frac{\partial (I_{\mathrm{d}} \tau_{ki})}{\partial x_k} \right\rangle + \langle u''_{\mathrm{d}_i} (S_{M\mathrm{d}_i} - U_i S_{\rho_{\mathrm{d}}}) \rangle + (1/2) \langle u''_{\mathrm{d}_i} u''_{\mathrm{d}_i} S_{\rho_{\mathrm{d}}} \rangle - \tilde{k}_{\mathrm{d}} \langle S_{\rho_{\mathrm{d}}} \rangle, \tag{A.7}$$

where U_i is the instantaneous velocity in the two-phase system. The dispersed-phase fluctuating velocity u''_{d_i} is defined with respect to the density-weighted mean as

$$u''_{\mathrm{d}_i} = U_i - \langle \tilde{U}_{\mathrm{d}_i} \rangle. \tag{A.8}$$

Here, the density-weighted mean velocity in the dispersed phase is given as

$$\langle \widetilde{U}_{\mathrm{d}_i} \rangle = \frac{\langle I_{\mathrm{d}} \rho U_i \rangle}{\langle I_{\mathrm{d}} \rho \rangle},$$

where ρ is the density of the two-phase flow field. The corresponding equations for the fluid phase are obtained by replacing d by f. In the above equations, I_{d} is the indicator function which is unity in the dispersed phase and zero in the fluid phase. The interphase momentum transfer $S_{M\mathrm{d}_i}$ is (Subramaniam, 2003; Xu, 2004)

$$S_{M\mathrm{d}_i} = \rho U_i \left(U_j - U_j^{(I)} \right) \frac{\partial I_{\mathrm{d}}}{\partial x_j} - \tau_{ji} \frac{\partial I_{\mathrm{d}}}{\partial x_j}, \tag{A.9}$$

where $U_j^{(I)}$ is the interface velocity (for example, the regression velocity of the droplet surface) and τ_{ji} is the stress tensor in the dispersed phase. The presence of $\partial I_{\mathrm{d}}/\partial x_j$ in the terms on the right-hand side imply that such terms are defined only at the interface. The interphase mass transfer term $S_{\rho_{\mathrm{d}}}$ can be written as (Subramaniam, 2003; Xu, 2004)

$$S_{\rho_{\mathrm{d}}} = \rho (U_i - U_i^{(I)}) \frac{\partial I_{\mathrm{d}}}{\partial x_i}. \tag{A.10}$$

With no interphase mass transfer, Eq. (A.7) simplifies to

$$\theta_d \rho_{\mathrm{d}} \frac{\mathrm{d}}{\mathrm{d}t}\tilde{k}_{\mathrm{d}} = \left\langle u''_{\mathrm{d}_i} \frac{\partial (I_{\mathrm{d}} \tau_{ki})}{\partial x_k} \right\rangle + \langle u''_{\mathrm{d}_i} S_{M\mathrm{d}_i} \rangle. \tag{A.11}$$

The correspondence between the dispersed-phase TKE evolution equation in the LE and EE representations is given below by comparing the right-hand sides of Eqs. (A.5) and (A.7)

$$2\left\langle u''_{\mathrm{d}_i} \frac{\partial (I_{\mathrm{d}} \tau_{ki})}{\partial x_k} \right\rangle + 2\langle u''_{\mathrm{d}_i} (S_{M\mathrm{d}_i}) \rangle \leftrightarrow \frac{4}{3} \pi \rho_{\mathrm{d}} n \langle R^3 \rangle 2 \widetilde{\langle A_i v''_i \rangle}$$

$$\langle u''_{\mathrm{d}_i} u''_{\mathrm{d}_i} S_{\rho_{\mathrm{d}}} \rangle \leftrightarrow \frac{4}{3} \pi \rho_{\mathrm{d}} n \langle R^3 \rangle \left(3 \widetilde{\langle v''_i v''_i \Gamma | t \rangle} \right)$$

$$-2\tilde{k}_{\mathrm{d}} \langle S_{\rho_{\mathrm{d}}} \rangle \leftrightarrow -\frac{4}{3} \pi \rho_{\mathrm{d}} n \langle R^3 \rangle \widetilde{\langle v''_i v''_i \rangle} (6 \langle \tilde{\Gamma} | t \rangle).$$

where $\leftrightarrow$ denotes the correspondence between the terms. For the case with zero interphase mass transfer, the correspondence simplifies to

$$\left\langle u''_{\mathrm{d}_i} \frac{\partial (I_{\mathrm{d}} \tau_{ki})}{\partial x_k} \right\rangle + \langle u''_{\mathrm{d}_i} (S_{M\mathrm{d}_i}) \rangle \leftrightarrow \frac{4}{3} \pi \rho_{\mathrm{d}} n \langle R^3 \rangle \widetilde{\langle A_i v''_i \rangle}.$$

Using DLM, the terms on the right-hand side involving Γ are in closed form since such terms can be easily computed from the solution. The above development enables one to estimate from the LE representation the corresponding unclosed term in the EE representation.

Appendix B. Mean droplet reynolds number estimate from DLM

Using standard methods to solve a time-dependent Ornstein–Uhlenbeck process (Gardiner, 1983) one can show that for a stochastic differential equation of the form

$$\mathrm{d}U(t) = -A(t)U(t)\mathrm{d}t + B(t)\mathrm{d}W(t), \tag{B.1}$$

where $A(t)$ and $B(t)$ are the drift and diffusion terms, respectively, and $\mathrm{d}W(t)$ is a Wiener process, the pdf of $U(t)$ is Gaussian with the mean and variance evolving according to

$$\langle U(t)\rangle = \mu \exp\left[-\int_0^t A(t')\mathrm{d}t'\right] \tag{B.2}$$

$$\mathrm{Var}[U(t)] = \sigma^2 \exp\left[-2\int_0^t A(t')\mathrm{d}t'\right] + \int_0^t \exp\left[-2\int_{t'}^t A(s)\mathrm{d}s\right] B^2(t')\mathrm{d}t', \tag{B.3}$$

for an initial Gaussian velocity field $U(t)$ with mean μ and variance σ^2. Note that Eqs. (3) and (4) are of the same form as Eq. (B.1).

One can then derive the probability density function of the absolute value of the relative velocity $\mathbf{W} = |\mathbf{u} - \mathbf{v}|$ as

$$f_W(w) = \sqrt{\frac{2}{\pi}}\left(\frac{2}{3}S\right)^{-3/2} w^2 \exp\left(-w^2 \Big/ \left[\frac{4}{3}S\right]\right),$$

where

$$S = k_\mathrm{f}(t) + k_\mathrm{d}(t) - 2\rho(t)\sqrt{k_\mathrm{f}(t)k_\mathrm{d}(t)}$$

and

$$\rho(t) = \frac{\langle u(t)v(t)\rangle}{\sqrt{\langle u(t)^2\rangle\langle v(t)^2\rangle}} = \frac{\langle u(t)v(t)\rangle}{\frac{2}{3}\sqrt{k_\mathrm{f}(t)k_\mathrm{d}(t)}}$$

is the correlation coefficient between like components of velocities u and v.[10] The mean of the absolute relative velocity W at any time t is

$$\langle W\rangle(t) = \frac{4}{\sqrt{3\pi}}\sqrt{S}.$$

So, the analytical mean droplet Reynolds number as implied by DLM for the non-evaporating case is

$$\langle Re_\mathrm{d}\rangle(t) = \frac{\langle W\rangle d_\mathrm{p}}{\nu_\mathrm{f}} = \frac{4}{\sqrt{3\pi}}\sqrt{S}\frac{d_\mathrm{p}}{\nu_\mathrm{f}} = \frac{4\sqrt{6}}{\sqrt{\pi}}St_\eta\sqrt{\left(\frac{\tau}{\tau_\mathrm{p}}\right)\left(1 + \frac{k_\mathrm{d}(t)}{k_\mathrm{f}(t)} - 2\rho(t)\sqrt{\frac{k_\mathrm{d}(t)}{k_\mathrm{f}(t)}}\right)\left(\frac{\rho_\mathrm{f}}{\rho_\mathrm{d}}\right)}. \tag{B.4}$$

The above expression shows that $\langle Re_\mathrm{d}\rangle$ can be written as a function of Stokes number St_η, ratio of τ ($=k_\mathrm{f}/\varepsilon_\mathrm{f}$) and particle response time τ_p, and the $k_\mathrm{d}/k_\mathrm{f}$ ratio. The same expression is true when a system reaches stationarity, where $k_\mathrm{f}(t) = k_\mathrm{f}^\mathrm{e}$ and $k_\mathrm{d}(t) = k_\mathrm{d}^\mathrm{e}$. It can be shown that the correlation coefficient $\rho(t)$ decreases exponentially to zero for DLM.

Using the analytical expression for the variance Eq. (B.3), one can compute the ratio $k_\mathrm{d}^\mathrm{e}/k_\mathrm{f}^\mathrm{e}$ for various Stokes numbers, which are in fact close to the DLM predictions reported in Fig. 3. For a Stokes number $St_\eta = 5$, the ratio $k_\mathrm{d}^\mathrm{e}/k_\mathrm{f}^\mathrm{e} \sim 0.52$. Substituting this value in the expression for $\langle Re_\mathrm{d}\rangle$ above, along with $k_\mathrm{f} = k_\mathrm{f}^\mathrm{e} = 1.5u'^2$ and the other non-dimensional ratios, the magnitude of $\langle Re_\mathrm{d}\rangle \sim 1.97$, which matches with DLM predictions. Thus, predictions from DLM are consistent with analytical results.

Appendix C. Asymptotic diffusion coefficient estimate from DLM

For the droplet-laden stationary turbulence case considered in this study, an analytical solution to the evolution of the dispersed phase velocity autocovariance given by Eq. (11) can be derived as follows. If we assume that the fluid-phase TKE k_f and the fluid-phase dissipation ε_f remain constant in artificially forced turbulence, then the eddy turnover time τ remains constant. Owing to the constant τ_p in the non-evaporating case and

[10] Since the turbulence is isotropic, $\rho(t)$ is the same for all the three like components of velocities.

constant τ_η the Stokes number St_η remains constant. Consequently, τ_3 remains constant in time. The analytical solution to Eq. (11) is thus (dropping the subscripts i for brevity)

$$\langle v(t_s)v(t)\rangle = \langle v(t_s)v(t_s)\rangle \mathrm{e}^{-t/(2\tau_3)}$$

where $t > t_s$ and t_s is the time at which the system reaches stationarity. Substituting the above expression into Eq. (12) and in the limit $t \to \infty$

$$\alpha_\mathrm{d}(\infty) = 2\langle v(t_s)v(t_s)\rangle\tau_3 = \frac{4}{3}k_\mathrm{d}(t_s)\tau_3 = \frac{4}{3}k_\mathrm{f}^\mathrm{e}\left(\frac{k_\mathrm{d}^\mathrm{e}}{k_\mathrm{f}^\mathrm{e}}\right)\tau_3.$$

The substitution $k_\mathrm{d}(t_s) = k_\mathrm{d}^\mathrm{e}$ has been made in the above development. Using the expression for analytical variance derived in Appendix B, one can compute the ratio of equilibrium TKE $k_\mathrm{d}^\mathrm{e}/k_\mathrm{f}^\mathrm{e}$. For $St_\eta = 5$, it is found that $\tau_3 = 56.9$ and $k_\mathrm{d}^\mathrm{e}/k_\mathrm{f}^\mathrm{e} = 0.57$, for which scaled $\alpha_\mathrm{d} = 1.15$. For $St_\eta = 0.4$, it is found that $\tau_3 = 44.8$ and $k_\mathrm{d}^\mathrm{e}/k_\mathrm{f}^\mathrm{e} = 0.97$, for which scaled $\alpha_\mathrm{d} = 1.54$. Both these values for analytical α_d are close to predictions from DLM.

The reason for the large magnitude of α_d compared to DNS results, especially at small Stokes numbers, lies in limiting value of τ_3 reached as $St_\eta \to 0$. In this limit, τ_3 evaluates to $[(3/2)C_0(\varepsilon_\mathrm{f}/k_\mathrm{f})]^{-1}$, since $1/\tau_1 \to 0$ in the one-way coupled limit assumed in this study. In this limit and for the parameters used in this study, the magnitude of $\tau_3 = 43.2$ and the corresponding dispersion coefficient $\alpha_\mathrm{d}(\infty) = 1.536$. These results are consistent with the predictions from DLM. It is noteworthy that in the limit $St_\eta \to 0$, $2\tau_3$ evaluates to the Lagrangian integral timescale (LIT) in the gas phase (Pope, 2000), and $\alpha_\mathrm{d}(\infty) = \alpha_\mathrm{f}(\infty)$ (cf. Fig. 5). It has been verified in the DNS of Yeung and Pope (1989) (see also Pope (2000)) that the SLM specification of the drift coefficients gives reasonable estimates for the LIT in the range of $Re_\lambda = 40 - 60$, which is the range of Re_λ studied in the DNS. However, no information on the LIT is reported by the DNS (Mashayek et al., 1997) used in this study for any quantitative comparisons of this timescale to be made.

References

Abramowitz, M., Stegun, I.A., 1964. Handbook of Mathematical Functions with Formulas, Graphs, and Mathematical Tables. Dover, New York.

Amsden, A.A., O'Rourke, P.J., Butler, T.D., 1989. KIVA-II: A Computer Program for Chemically Reactive Flows with Sprays. Tech. Rep. LA-11560-MS, Los Alamos National Laboratory.

Batchelor, G.K., 1971. An Introduction to Fluid Dynamics. Cambridge University Press, Port Chester, NY.

Boivin, M., Simonin, O., Squires, K., 1998. Direct numerical simulation of turbulence modulation by particles in isotropic turbulence. J. Fluid Mech. 375, 235–263.

Chagras, V., Oesterle, B., Boulet, P., 2005. On the heat transfer in gas–solid pipe flows: Effects of collision induced alterations of the flow dynamics. Int. J. Heat Mass Transfer 48, 1649–1661.

Chen, X.-Q., Pereira, J.C.F., 1997. Efficient computation of particle dispersion in turbulent flows with a stochastic-probabilistic model. Int. J. Heat Mass Transfer 40, 1727–1741.

Clift, R., Grace, J.R., Weber, M.E., 1978. Bubbles, Drops and Particles. Academic Press, New York.

Csanady, G.T., 1963. Turbulent diffusion of heavy particles in the atmosphere. J. Atmos. Sci. 20, 201–208.

Drew, D.A., 1983. Mathematical modeling of two-phase flow. Annu. Rev. Fluid Mech. 15, 261–291.

Faeth, G.M., 1977. Current status of droplet and liquid combustion. Prog. Energy Combust. Sci. 3, 191–224.

Gao, Z., Mashayek, F., 2004a. Stochastic model for nonisothermal droplet-laden turbulent flows. AIAA J. 42, 255–260.

Gao, Z., Mashayek, F., 2004b. Stochastic modeling of evaporating droplets polydis-persed in turbulent flows. Int. J. Heat Mass Transfer 47, 4339–4348.

Gardiner, C.W., 1983. Handbook of Stochastic Methods. Springer, New York.

Gosman, A.D., Ioannides, E., 1983. Aspects of computer simulation of liquid fueled combustors. J. Energy 6, 482–490.

Gouesbet, G., Berlemont, A., 1999. Eulerian and Lagrangian approaches for predicting the behaviour of discrete particles in turbulent flows. Prog. Energy Combust. Sci. 25, 133–159.

Gouesbet, G., Picart, A.B., 1984. Dispersion of discrete particles by continuous turbulent motions. Extensive discussion of the Tchen's theory, using a two-parameter family of Lagrangian correlation functions. Phys. Fluids 27, 827–837.

Greene, G.A., Irvine, T.F., Gyves, J., Smith, T., 1993. Drag relationships for liquid droplets settling in a continuous liquid. A.I.Ch.E.J. 29, 37–41.

Groszmann, D.E., Rogers, C.B., 2004. Turbulent scales of dilute particle-laden flows in microgravity. Phys. Fluids 16, 4671–4684.

Haworth, D.C., Pope, S.B., 1986. A generalized Langevin model for turbulent flows. Phys. Fluids 29, 387–405.

Hinze, J.O., 1975. Turbulence, 2nd ed. McGraw-Hill series in Mechanical Engineering, New York.

Kloeden, P., Platen, E., 1992. Numerical Solution of Stochastic Differential Equations. Springer, New York.

Lu, Q.Q., 1995. An approach to modeling particle motion in turbulent flows – I. Homogeneous, isotropic turbulence. Atmos. Environ. 29, 423–436.

Mashayek, F., 1998. Droplet–turbulence interactions in low-Mach number homogeneous shear two-phase flows. J. Fluid Mech. 367, 163–203.

Mashayek, F., 1999. Stochastic simulations of particle-laden isotropic turbulent flow. Int. J. Multiphase Flow 25, 1575–1599.

Mashayek, F., Jaberi, F.A., Miller, R.S., Givi, P., 1997. Dispersion and polydispersity of droplets in stationary isotropic turbulence. Int. J. Multiphase Flow 23, 337–355.

Maxey, M.R., Riley, J.J., 1983. Equation of motion for a small rigid sphere in a non-uniform flow. Phys. Fluids 26, 883–889.

Pai, M.G., Subramaniam, S., 2006. Modeling interphase turbulent kinetic energy transfer in Lagrangian–Eulerian spray computations. Atomization and Sprays 16, 807–826.

Pope, S.B., 1985. PDF methods for turbulent reactive flows. Prog. Energy Combust. Sci. 11, 119–192.

Pope, S.B., 2000. Turbulent Flows. Cambridge University Press, Port Chester, NY.

Pozorski, J., Minier, J.-P., 1999. Probability density function modeling of dispersed two-phase turbulent flows. Phys. Rev. E 59, 855–863.

Ranz, W.E., Marshall, W.R., 1952. Evaporation from drops. Parts I and II. Chem. Eng. Prog. 48, 141–146, 173–180.

Snyder, W.H., Lumley, J.L., 1971. Some measurements of particle velocity autocorrelation functions in a turbulent flow. J. Fluid Mech. 48, 41–71.

Squires, K.D., Eaton, J.K., 1991. Measurements of particle dispersion obtained from direct numerical simulations of isotropic turbulence. J. Fluid Mech. 226, 1–35.

Subramaniam, S., 2000. Statistical representation of a spray as a point process. Phys. Fluids 12, 2413–2431.

Subramaniam, S., 2001. Statistical modeling of sprays using the droplet distribution function. Phys. Fluids 13, 624–642.

Subramaniam, S., 2003. Modeling Turbulent Two-phase flows. In: Proceedings of the Sixteenth Annual Conference on Liquid Atomization and Spray Systems. International Liquid Atomization and Spray Systems Soc.

Sundaram, S., Collins, L.R., 1999. A numerical study of the modulation of isotropic turbulence by suspended particles. J. Fluid Mech. 379, 105–143.

Tchen, C.M., 1947. Mean value and correlation problems connected with the motion of small particles suspended in a turbulent fluid. Ph.D. thesis, University of Delft, The Hague.

Ten Cate, A., Derksen, J.J., Portela, L.M., Van Den Akker, H.E.A., 2004. Fully resolved simulations of colliding monodisperse spheres in forced isotropic turbulence. J. Fluid Mech. 519, 233–271.

Truesdell, G.C., Elghobashi, S., 1994. On the two-way interaction between homogeneous turbulence and dispersed solid particles. II. Particle dispersion. Phys. Fluids 6, 1405–1407.

Warnica, W.D., Renksizbulut, M., Strong, A.B., 1995a. Drag coefficients of spherical liquid droplets Part 1: Quiescent gaseous fields. Exp. Fluids 18, 258–264.

Warnica, W.D., Renksizbulut, M., Strong, A.B., 1995b. Drag coefficients of spherical liquid droplets Part 2: Turbulent gaseous fields. Exp. Fluids 18, 265–276.

Wells, M.R., Stock, D.E., 1983. The effects of crossing trajectories on the dispersion of particles in a turbulent flow. J. Fluid Mech. 136, 31–62.

Williams, F.A., 1958. Spray combustion and atomization. Phys. Fluids 1, 541–545.

Xu, Y., 2004. An improved multiscale model for dilute turbulent gas particle flows based on the equilibration of energy concept. Master's thesis, Iowa State University, USA.

Xu, Y., Subramaniam, S., 2006. A multiscale model for dilute turbulent gas-particle flows based on the equilibration of energy concept. Phys. Fluids 18, 033301.

Yeung, P.K., Pope, S.B., 1989. Lagrangian statistics from direct numerical simulations of isotropic turbulence. J. Fluid Mech. 207, 531–586.